# Study on precision pressure measurement of ultra high-pressure gas

Hideaki Iizumi

February 2021

# Study on precision pressure measurement of ultra high-pressure gas

Hideaki Iizumi

Doctoral Program in Physics

Submitted to the

Degree Programs in Pure and Applied Sciences of the

Graduate School of Science and Technology

in Partial Fulfillment of the Requirements

for the Degree of Doctor of Philosophy in

Science

at the

University of Tsukuba

# Contents

# 1. Introduction

The measurement of pressure is one of the essential measurements in society, industry, and science and technology [1]. The pressure measurements for safety and security include the atmospheric measurement in meteorological observation, the altitude measurement for aircrafts, the blood pressure in medicine and health management, the measurement for high-pressure gas control, and the pressure measurement in the manufacturing process. The pressure measurements for energy savings include the air conditioning of buildings and the adjustment of air pressure in tires and automobile engines. Moreover, various pressure measurements are conducted at various sites such as the maintenance of clean rooms where high air purity must be maintained for the manufacture of semiconductors and precision devices, the measurement and control of pressure in various processing, and the inspection of plants. In the field of science and technology, various R&Ds using pressure control and measurements are being done.

Recently, Activities to reduce greenhouse gases have been promoted. For the realization of hydrogen society that does not emit greenhouse gases, fuel cell vehicles have been promoted. The Ministry of Economy, Trade and Industry has set a goal of popularizing 200,000 fuel cell vehicles, and developing 320 hydrogen stations by 2025 in Strategic Roadmap for Hydrogen and Fuel Cells. The Japanese government has declared a policy to reduce greenhouse gas emissions to net zero by 2050, that is, to realize carbon-neutral, carbon-free society. The use of hydrogen energy has become more important. Hydrogen gas used in fuel cell vehicles and hydrogen stations is stored at pressures exceeding 70 MPa for fuel efficiency. For safety control and quality control, pressure measurement of such ultra high-pressure gas is necessary. The demands for pressure measurements of ultra high-pressure gas are expected to steadily increase as fuel cell vehicles become increasingly popular. Such pressure measurements are also important in other field where ultra high-pressure gas is used such as natural gas pipelines, industrial plants, and scientific research [2 - 5].

To ensure reliable and high precision measurements, pressure gauges must be calibrated regularly. But pressure standards for high-pressure gas have not been sufficiently established because the demand for measurement has been small so far and handle of high-pressure gas is difficult. National measurement standards of hydraulic pressure have been established for pressures up to 1 GPa. On the other hand, national measurement standards of gas pressure have been established for pressures up to 7 MPa. Since gas pressure standard of high pressure is not established, pressure gauges for ultra high-pressure gas are calibrated by hydraulic pressure standard. The purity of hydrogen is very important in fuel cell vehicles, and mixing the remaining liquid into hydrogen is a serious problem. The gas pressure standard of ultra high-pressure for directly calibrating gas pressure gauges is therefore strongly desired. A few countries have capabilities of the gas pressure calibration above 70 MPa. Only the United States and Germany have capabilities of the gas pressure calibration up to 100 MPa [6, 7].

The purpose of this study is establishment of the reliable and high precision pressure measurement of ultra high-pressure gas. For ensuring reliable measurements, we have developed a pressure calibration

system for pressure gauges measuring ultra high-pressure gas of pressures up to 100 MPa [8]. The developed calibration system is described in section 2. We explain the system components such as standard device, and pressure supply and control device. A liquid-lubricated pressure balance is evaluated for using as the standard device. Then, we show the calibration method and the calibration result of a pressure gauge. In order to confirm the consistency of the calibration results, a comparison with hydraulic pressure standard and an international comparison is performed. We show a discussion of the piston fall rate of the liquid-lubricated pressure balance. The fall rate of the piston is an important characteristic for operating pressure balances. Gas inside the pressure piping in the calibration system is compressed and expanded due to the pressure change. The temperature changes of gas are measured by a thermocouple during a stepwise calibration cycle.

To perform precision pressure measurements, it is necessary to periodically calibrate the pressure gauges and understand their characteristics such as hysteresis and temperature dependence [9 - 14]. Although different industries utilize a wide variety of gasses, the pressure gauges used in high-pressure gas applications are generally calibrated using an inert gas, such as nitrogen. However, the calibration value of pressure gauges might be affected by the type of gas used, which has not been clarified yet, and thus needs some correction especially for gases having different properties, such as hydrogen used at hydrogen stations and fuel-cell vehicles.

The effect of pressure transmitting medium on quartz Bourdon-type pressure transducers [15 - 17] is evaluated in this study by using the developed calibration system [18 - 20]. The pressure transducers are used in precision high-pressure measurements as a secondary standard. They are important in the traceability chain of the high pressure. In an international comparison, the pressure transducers were used as a transfer standard. Gas pressure standards for pressures up to 100 MPa of each country were compared in the international comparison [21]. The international comparison was conducted for ensuring international equivalence of developed gas pressure standard. The pressure medium was nitrogen in our institute, and was helium in the United States in the international comparison. The standard device of the United States was different type with our standard device [7]. The United States used helium due to the specifications of standard device. Therefore, the transfer standard was calibrated by using nitrogen and helium in our institute beforehand. The calibration values of the pressure transducers changed depending on the type of pressure medium used. The trend and amount of the effect was different for the two transducers. This result showed the calibration values of the pressure transducers was affected by the type of measuring gas. The difference between the calibration values by using nitrogen and that by using helium was comparable to the claimed uncertainties of each country and was not negligible in the international comparison. The calibration values calibrated by using helium were corrected to the values using nitrogen according to the evaluation result. The results of the comparison finally showed good agreement. However, the reason for the effect of type of gas is still unclear. Determining the effects of the type of gas on the pressure transducer is important for both precision measurements and the traceability chain of high pressure.

In section 3, the effect of the type of gas on the calibration values of the quartz Bourdon-type pressure transducer is evaluated in detail with developed calibration system. The reason for the effect is investigated with a focus on the gas density and the structure of the sensing element. To confirm the assumption of the reason experimentally, the effect of the orientation of the pressure transducer is evaluated. We also evaluate the relationship between the level of variation and the density of gas, using a total of six different gas densities: argon, nitrogen, helium, and three types of mixed gases. Because the density in actual measurement condition is necessary, the density of the high-pressure gas is measured in-situ by measuring head differential pressure.

Based on the above evaluation results, the methods for reducing the variations is described in section 4. When the transducers are mounted horizontally, the variation due to the type of gas is reduced by adjusting the rotation angle of the transducer around its central axis. We introduce an appropriate arrangement of two transducers, with which the effects of both the type of gas and the orientation of the transducer are highly reduced. We also discuss a method for estimating the calibration values from gas density. Finally, a summary of this study is given in section 5.

# 2. Development of calibration system for pressure gauges measuring ultra high-pressure gas

## 2.1 Pressure calibration system for ultra high-pressure gas

To ensure reliable measurements, pressure gauges must be calibrated regularly. National measurement standards of gas pressure have been established for pressures up to 7 MPa. The demand for pressure measurement of ultra high-pressure gas has been increasing in recent years. For ensuring reliable pressure measurements of ultra high-pressure gas, we have developed a gas pressure calibration system for pressure gauges measuring ultra high-pressure gas. The calibration system is introduced and evaluated in section 2. The developed pressure calibration system for pressures up to 100 MPa is shown in Fig. 2.1. A liquid-lubricated pressure balance is used as standard device. The main components of this system are the liquid-lubricated pressure balance, an automatic weight handler, a gas pressure controller, a variable volume, a gas booster, and an environmental measuring device. The liquid-lubricated pressure balance can be calibrated from the comparison against the hydraulic pressure standard. Comparative calibration is performed by applying the same pressure to the liquid-lubricated pressure balance and the device under calibration. The device under calibration is calibrated by comparing the output value with the value of the standard device.
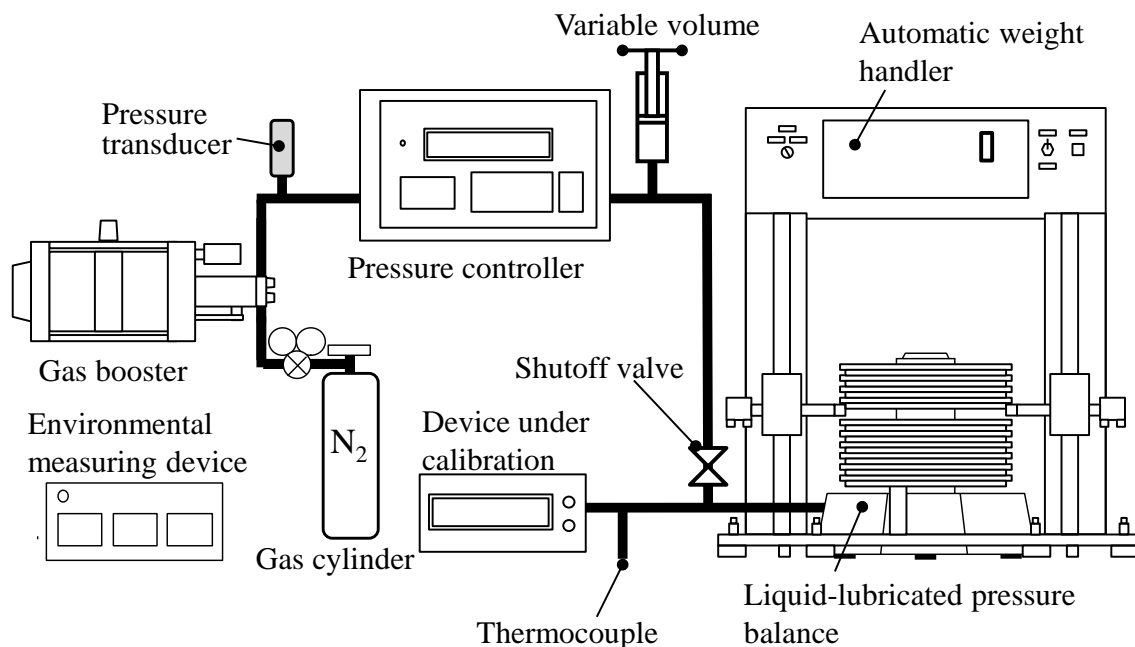


Figure 2.1.   Gas pressure calibration system for pressures up to 100 MPa. A liquid-lubricated pressure balance is a standard device. Comparative calibration is performed by applying the same pressure to the standard device and the device under calibration.

4

## 2.1.1  Standard device

A pressure balance is commonly used as a pressure standard device. The mainly component of the pressure balance is a piston-cylinder and weights as shown in Fig. 2.2. The pressure balance can generate stable pressure and has excellent long-term stability [22 - 33]. The generated pressure of the pressure balance can be calculated by dividing the gravitational force due to the mass of the piston and weights by the effective area of the piston-cylinder, according to the definition of pressure. When a downward gravitational force due to the mass of the piston and weights is balanced with an upward force due to the applied pressure, the piston floats in the cylinder. To eliminate mechanical contact between the piston and the cylinder, the piston rotates inside the cylinder during operation. The piston falls at a specific speed owing to the leakage of the pressure transmitting medium through the gap between the piston and the cylinder. During the piston floats at an appropriate position inside the cylinder, the generated pressure is highly stable and accurately evaluated.

Surfaces of piston and cylinder are precisely machined and the gap between the piston and the cylinder is less than 1 μm. If the gap is too large, the leakage of the pressure medium through the gap increase, and the piston will fall too fast to generate stable pressure. If the gap is too narrow, the piston and the cylinder can make contact due to the pressure distortion. In either case, the stable pressure cannot be generated. The gap of the gas piston-cylinder is usually narrower than that of hydraulic ones, because gas viscosities are lower than those of liquids and gas leaks easily through the gap. The piston-cylinders for high-pressure applications furthermore require small diameters. It is difficult to machine a piston-cylinder for ultra high-pressure gas.

There are several types of the piston-cylinders, which can be used according to the application and the pressure range. As a typical example, Fig. 2.3 shows a conceptual diagram of a simple type, a re-entrant type, and a controlled-clearance type piston-cylinder. The simple type is commonly used and is relatively easy to design and operate. The re-entrant type and the controlled-clearance type are used for high pressure. The re-entrant type has a structure in which the cylinder is tightened due to the generated pressure is also applied to the outer surface. It is possible to suppress the deformation of the cylinder under high pressure and prevent an excessive leakage of the pressure medium. In the controlled-clearance type, a jacket pressure given from a pressure source independent of the generated pressure is applied to the outer surface of the cylinder, and the clearance between the piston and the cylinder can be actively controlled. Although the structure and the operation are complicated, the pressure change of the effective area can be evaluated independently without comparison with other standard devices.
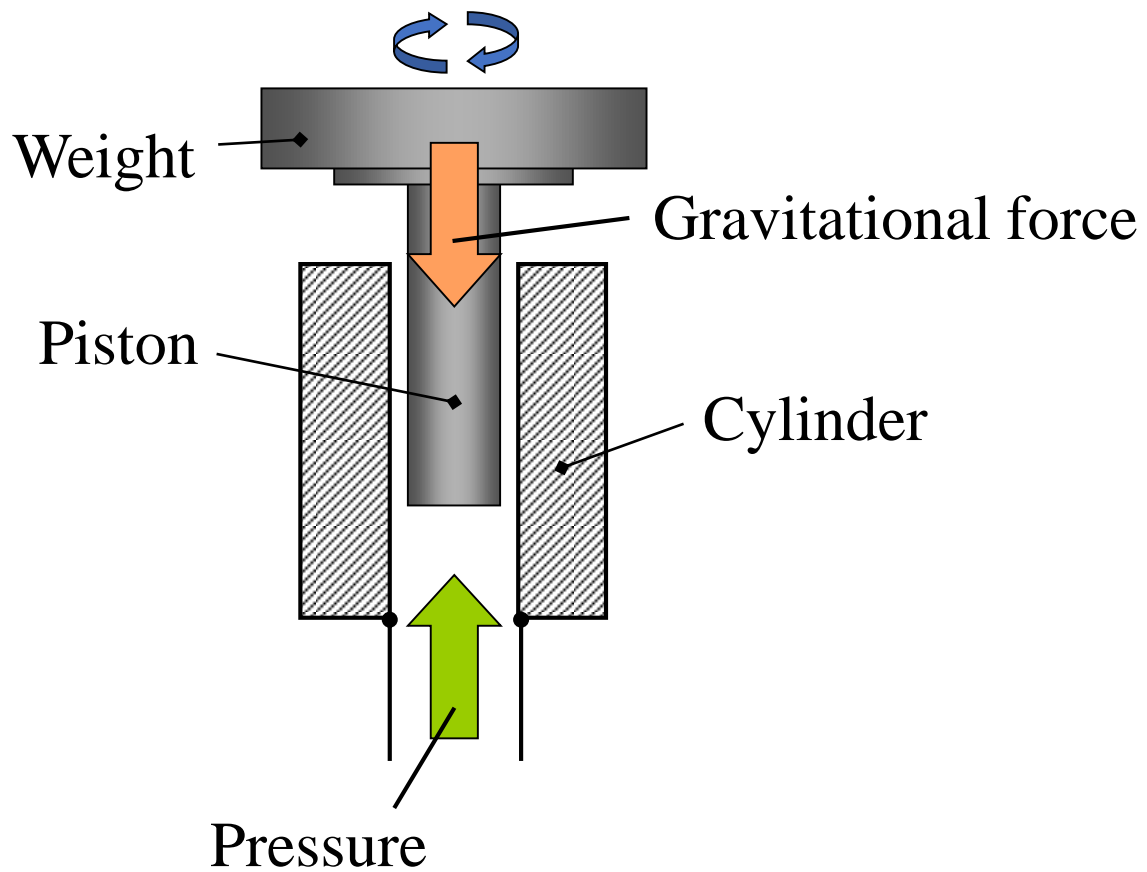
Figure 2.2. Schematic drawing of pressure balance. The main components are a piston, a cylinder and weights.
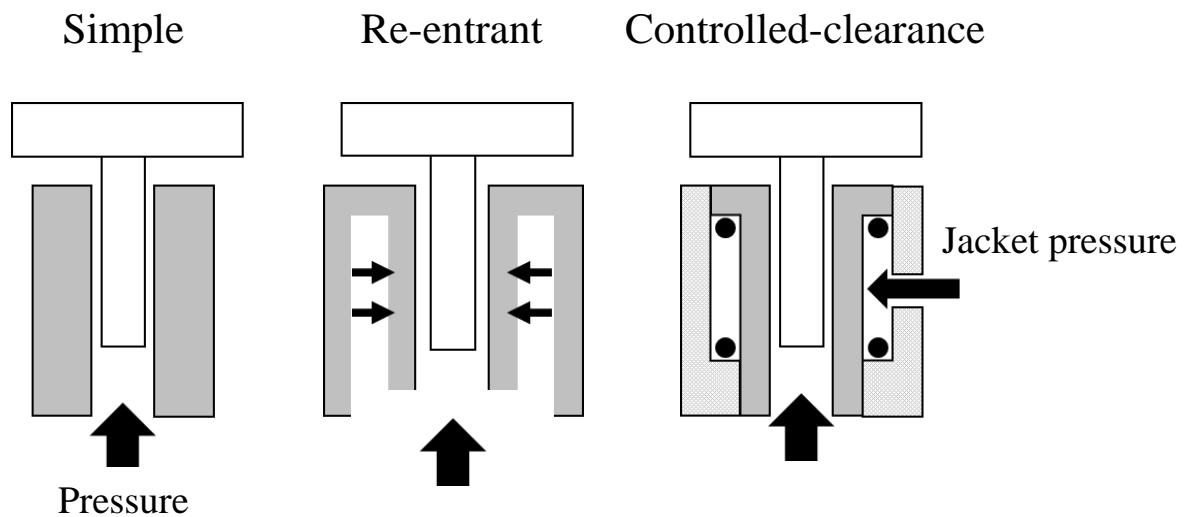


Figure 2.3. Conceptual diagram of a simple type, a re-entrant type, and a controlled-clearance type piston-cylinders.

The liquid-lubricated gas pressure balance, manufactured by Fluke Calibration (PG7202) [34, 35] can generate stable gas pressures up to 100 MPa. Fig. 2.4 shows a sectional drawing of the piston-cylinder assembly of the liquid-lubricated pressure balance. This pressure balance can generate both gas pressure and hydraulic pressure. A feature of the pressure balance is the reservoir is located outside the cylinder. The reservoir is connected to the clearance between the piston and the cylinder through two holes in the cylinder. Therefore, the piston-cylinder clearance is filled with liquid. The clearance of the liquid-lubricated piston-cylinder is similar to that of a hydraulic one.

When the gas inside the piston-cylinder assembly is removed and the piston-cylinder assembly is filled with liquid, hydraulic pressure can be generated by the liquid-lubricated pressure balance. The effective area of the liquid-lubricated piston-cylinder when gas pressure is generated is theoretically the same as that when hydraulic pressure is generated. It is confirmed experimentally that the effective area of the liquid-lubricated piston-cylinder when gas pressure is generated and that when hydraulic pressure is generated are consistent up to 7 MPa [34]. Dioctyl sebacate is commonly used as pressure medium of hydraulic pressure calibration, and is used in the reservoir and hydraulic pressure medium in this study.
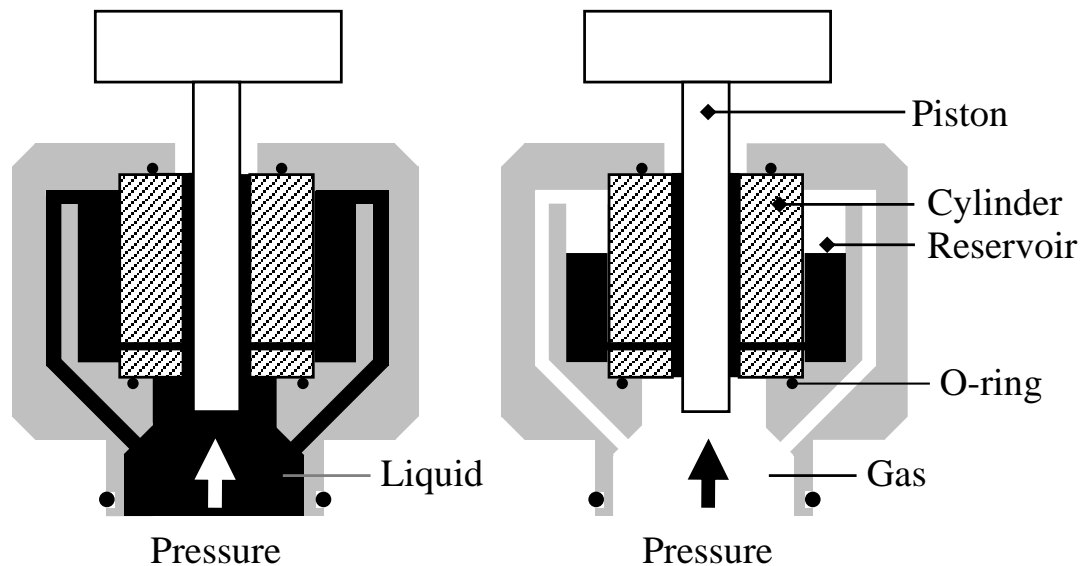


Figure 2.4. Schematic drawing of liquid-lubricated piston-cylinder assembly

## 2.1.2  Calibration equipment

Each equipment of the developed calibration system is described, in the following. The pressure transmitting medium of the developed calibration system is nitrogen gas. The pressure supply source is the gas cylinder which is initially pressurized to about 14 MPa. The nitrogen gas from the gas cylinder is pressurized to about 100 MPa by a gas booster which is driven by compressed air. A compression ratio of the gas booster is 25:1. A pressure transducer measures the outlet pressure of the gas booster for feedback control. When the outlet pressure reaches the set pressure, feedback control via a computer

automatically closes a shut-off valve installed in the compressed air line which is used for driving the gas booster, and the gas booster stops pressurization of nitrogen gas. The set pressure is determined based on the maximum calibration pressure. Nitrogen gas is supplied to a pressure controller after pressuring by the gas booster. The pressure controller is used to supply accurately adjusted and sufficiently stable gas pressure to the standard device and the device under calibration. The pressure controller can automatically control the floating position of the piston through fine pressure adjustments by communicating with the pressure balance. A variable volume is also used to manually adjust the floating position of the piston. After adjusting the floating position of the piston, the shut-off valve is closed to be more stable the pressure applied to the liquid-lubricated pressure balance and device under calibration. The calibration is conducted by comparing the applied pressure from the liquid-lubricated pressure balance with the output value of the device under calibration.

The environmental temperature, humidity, and atmospheric pressure are measured by the environmental measuring device for mass buoyancy correction and to calculate the absolute pressure. In this study, a sheathed thermocouple is inserted into the piping to measure the temperature change due to the adiabatic process during a calibration. The generated pressure of the pressure balance can be determined by changing the weights to be loaded. An automatic weight handler is used to load and unload the weights of the pressure balance. The set of weights used consists of a 4 kg weight, a 5 kg weight, and nine 10 kg weights. The total mass, including the piston and bell type weight, is 100 kg. All equipment in the calibration system can be operated from a computer. When the output value of the device under calibration can be obtained from the computer, fully automatic pressure calibration can be performed.

## 2.2 Generated pressure of pressure balance

During the piston floats at an appropriate position, the generated pressure is highly stable and accurately evaluated. The generated pressure of the pressure balance can be evaluated by dividing the gravitational force due to the mass of the piston and weights by the effective area of the piston-cylinder, according to the definition of pressure. The generated pressure $p$ at the pressure measuring position is given by the following equation including the correction coefficient.

$$ p = \frac{Mg\left(1 - \frac{\rho_a}{\rho_w}\right) + \gamma C}{A(0, t_r)(1 + \lambda p)\left[1 + \alpha(t - t_r)\right]} + (\rho_f - \rho_a)gH, \quad (2.1) $$

where $M$ is the total mass of the piston and weights, $\rho_w$ is the average density of the piston and weights, $\rho_a$ is air density, $g$ is gravitational acceleration at the measurement position, $\gamma$ is the surface tension of the pressure medium, $C$ is the piston circumference. The denominator is a term related to the effective area. $A(0, t_r)$ is the effective area under atmospheric pressure at reference temperature $t_r$, $\lambda$ is the pressure distortion coefficient, $\alpha$ is the sum of the thermal expansion coefficient of the piston and the cylinder, $t$ is

the temperature. The second term, $(\rho_f - \rho_a)gH$, is the correction term for the pressure difference due to the head difference. $\rho_f$ is the density of the pressure medium as a function of the generated pressure. $H$ is the height difference between the measurement position and the reference level of pressure balance, and is positive when the measurement position is relatively lower. The generated pressure can be calculated by evaluating these parameters.

Evaluation of the effective area of the piston-cylinder is the most important for the accurate evaluation of the generated pressure. The effective area is not a simply piston cross-sectional area but includes the effect of the clearance between the piston and the cylinder. There are two types of the evaluation methods for the effective area. One method is calculating based on the dimensional measurements and the material properties of the piston-cylinder. On the other hand, the effective area of the piston-cylinder also can be evaluated through comparison with a known generated pressure. As described in section 2.1.1, the effective area of the liquid-lubricated piston-cylinder when gas pressure is generated is theoretically the same as that when hydraulic pressure is generated. National measurement standards of hydraulic pressure have been established for pressures up to 1 GPa. This feature can be used to evaluate the effective area of the liquid-lubricated piston-cylinder through comparison with hydraulic pressure standard of the same pressure range. National measurement standards of hydraulic pressure have been ensured international equivalence at pressures up to 100 MPa by the interlaboratory comparisons [36, 37]. The traceable calibration of the liquid-lubricated pressure balance to national measurement standards can be performed.

Calibrations of the liquid-lubricated pressure balance were performed using the comparator method [38], which uses a precise pressure transducer and two constant-volume valves. The pressures generated by the standard pressure balance and the pressure balance under calibration are compared via the precise pressure transducer. The effective areas of a liquid-lubricated piston-cylinder was evaluated with this method and was shown in Fig. 2.5. A nominal effective area of the liquid-lubricated piston-cylinder is 9.8 mm$^2$ and maximum pressure is designed to be 100 MPa. The effective area at a reference temperature of 23 °C was shown in the vertical axis as a function of pressure. The effective area was evaluated from 10 MPa to 100 MPa at every 10 MPa step. An approximate straight line was also shown.

The effective area decreases almost linearly with pressure. The slope of the approximate straight line is the pressure distortion coefficient. The pressure distortion coefficient is negative ($-2.3 \times 10^{-6}$ MPa$^{-1}$). The pressure distortion coefficient of the simple type piston-cylinder is positive because the clearance between the piston and the cylinder become wide due to the pressure applying to the clearance. The liquid-lubricated piston-cylinder is the re-entrant type. The clearance of the re-entrant type piston-cylinder become narrow with pressure because the generated pressure is also applied to the outer surface of the cylinder.

The calibration value has the uncertainty, and the uncertainty of calibration values is also evaluated in the calibration. The uncertainty of the generated pressure can be estimated by considering all parameters used in calculation of the generated pressure as uncertainty components [39, 40]. Table 2.1 showed an uncertainty evaluation of the pressure generated at 100 MPa by the liquid-lubricated piston-cylinder. The standard uncertainties of the major parameters were listed in the table. Uncertainty

components whose effect on the generated pressure is relatively less than $1\times10^{-6}$ are disregarded. The uncertainty of the effective area evaluated by the hydraulic pressure standard is the main factor. Relative standard uncertainty of the generated pressure is estimated to be $1.8\times10^{-5}$ at 100 MPa. Fig. 2.6 shows the relative standard uncertainty of the generated pressure as a function of pressure. The uncertainty of the generated pressure increases with pressure due to the pressure distortion coefficient $\lambda$ of the effective area.
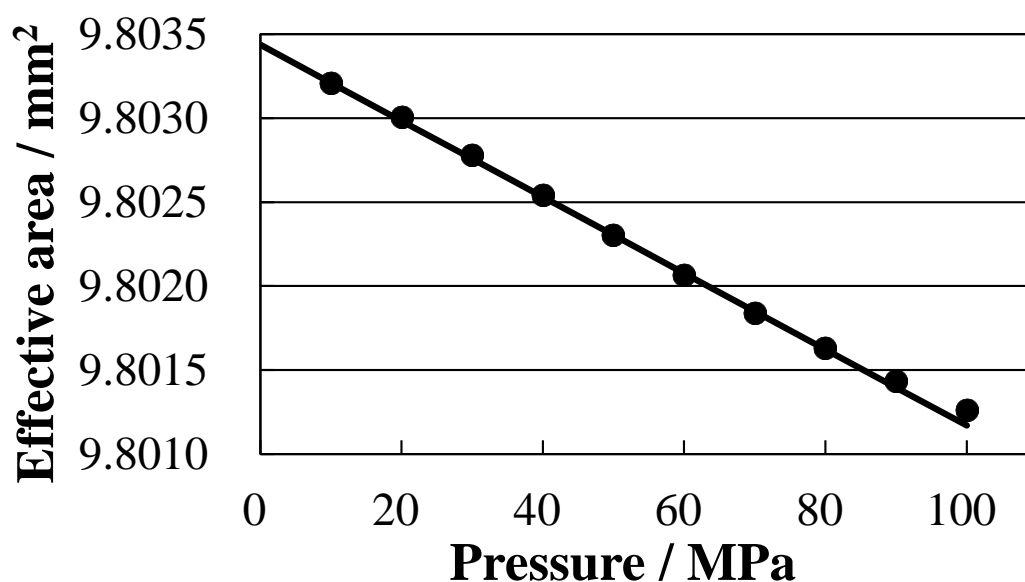


Figure 2.5. Effective area of a liquid-lubricated piston-cylinder evaluated by hydraulic pressure standard.

Table 2.1. Uncertainty components of pressure generated by liquid-lubricated piston-cylinder at 100 MPa. The uncertainty of the effective area evaluated by the hydraulic pressure standard is the main factor.

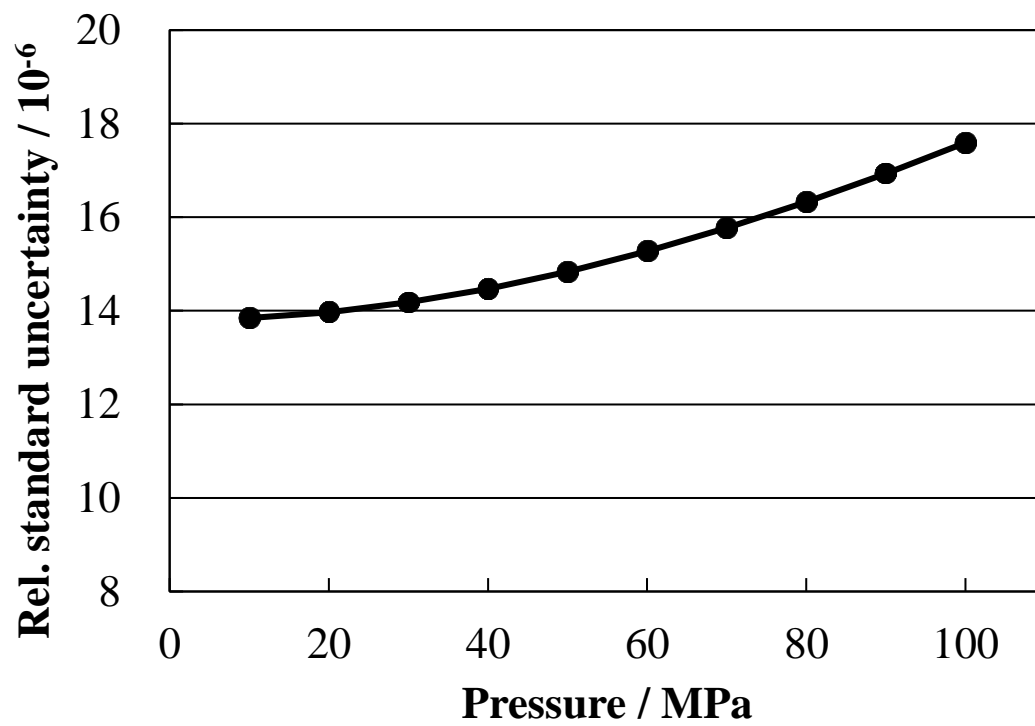| Components | Value | Standard uncertainty | Relative standard uncertainty /$10^{-6}$ |
|---|---|---|---|
| $A(0, t_r)$ | $9.8 \times 10^{-6}$ m$^2$ | $1.3 \times 10^{-10}$ m$^2$ | 13 |
| $\lambda$ | $-2.3 \times 10^{-6}$ MPa$^{-1}$ | $1.1 \times 10^{-7}$ MPa$^{-1}$ | 11 |
| $t$ | 23 °C | 0.2 °C | 1.8 |
| $M$ | 100 kg | 250 mg | 2.5 |
| Combined uncertainty | 100 MPa | 1.8 kPa | 18 |

Figure 2.6. Pressure dependence of relative standard uncertainty of generated pressure. The uncertainty of the generated pressure increases with pressure due to the pressure distortion coefficient of the effective area.

## 2.3 Calibration of pressure gauge by developed calibration system

### 2.3.1 Calibration method

Calibration is performed with the pressure generated by the liquid-lubricated pressure balance and its uncertainty evaluated in section 2.2. In this section, a quartz Bourdon-type pressure transducer [15] of maximum pressure 100 MPa was calibrated using the developed system. The quartz Bourdon-type pressure transducer is used for the precision measurement of high pressure. Comparative calibration is performed by applying the same pressure to the liquid-lubricated pressure balance and the pressure transducer. The pressure transducer is calibrated by comparing the output value with the value of the standard device. The calibration was performed automatically under computer control. The measurement pressure was from 0 MPa to 100 MPa at every 10 MPa step. After the measurement at 100 MPa is completed, measurement in descending process is performed at same measurement pressure with ascending process. There is a waiting time of 60 min between the ascending and descending processes. Immediately after the pressure is changed, the generated pressure is not stable due to the deformation of the pressure piping. At each measurement pressure, the output of the device under calibration was sampled 18 times at 10 sec intervals, after waiting at least seven minutes following establishment of a steady pressure. The average value of three cycles was calculated and used as the calibration value.

### 2.3.2 Calibration result of pressure gauge

Fig. 2.7 shows the calibration result of the quartz Bourdon-type pressure transducer using the method described in section 2.3.1. The vertical axis shows the deviation of the indication of the pressure transducer from the standard pressure. The indication and the standard pressure after offset correction were used for calculation. The value at each pressure was subtracted by the value at 0 MPa before calibration cycle. In the figure, solid lines showed the ascending process and dashed lines showed the descending process. The results of three calibration cycles were shown separately. The deviation of the indication of the pressure transducer from the standard pressure increased with pressure. The calibration curve showed maximum hysteresis at around 50 MPa. The indication of the pressure transducer in the descending process was larger than that in the ascending process.
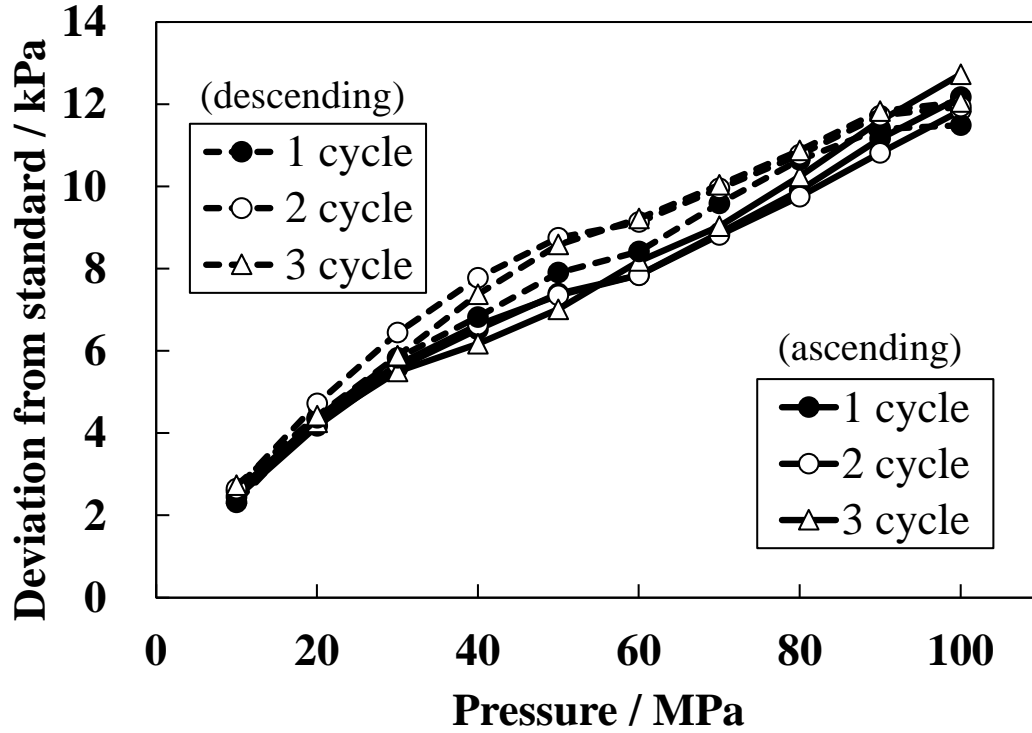
Figure 2.7. Calibration results of a pressure transducer by the developed gas pressure calibration system. Solid line shows ascending process and dashed line shows descending process. The results of three calibration cycles are shown separately.

The relative standard deviation of 18 outputs at each measurement pressure was less than $4\times10^{-6}$ at above 20 MPa. This result shows that the generate pressure of the developed calibration system is sufficiently stable. The standard deviation of data obtained over three cycles was less than 0.5 kPa at each measurement pressure, relatively $5\times10^{-6}$ of the maximum pressure. This standard deviation is sufficiently lower than the uncertainty of the generated pressure. It shows that the measurement repeatability of the pressure transducer is good.

In uncertainty evaluations of the calibration value, the uncertainty of generated pressure is dominant in this calibration. The relative expanded uncertainty ($k = 2$) of the calibration value is estimated to be $4\times10^{-5}$ at all measurement pressures. The expanded uncertainty ($k = 2$) is two times the standard uncertainty, and means an interval having a level of confidence of approximately 95 % [41]. The expanded uncertainty is commonly used in the calibration of measuring instrument.

## 2.4 Consistency of calibration result

## 2.4.1 Comparison with hydraulic pressure standard

The validity of the developed calibration system is described in this section. The effective area of the piston-cylinder was calibrated through the comparison with the hydraulic pressure. It has been confirmed that the effective area of the liquid-lubricated piston-cylinder when gas pressure is generated is consistent with that when hydraulic pressure is generated for pressures up to 7 MPa [34]. Here, it is confirmed that the calibration results by the developed gas pressure calibration system are consistent with those by an existing hydraulic pressure calibration system for pressures up to 100 MPa.

In section 2.3.2, the quartz Bourdon-type pressure transducer for pressures up to 100 MPa was calibrated by the developed calibration system. The same pressure transducer was also calibrated by the hydraulic pressure calibration system using same calibration procedure. Since silicon oil is filled in a pressure piping inside this pressure transducer, this pressure transducer can measure the pressure of both gas and liquid. Silicon oil is usually not filled in the gas pressure transducer because it may affect the purity of gas to be measured.

A pressure balance of hydraulic pressure which has the simple type piston-cylinder is used for hydraulic pressure calibration. Calibration results of the pressure transducer is shown in Fig. 2.8. The deviation from standard pressure after offset correction was shown. The calibration value at each pressure was subtracted by the value at 0 MPa before calibration cycle. In the figure, solid lines show the ascending process and dashed lines show the descending process. The results of three calibration cycles are shown separately. The standard deviation of the three data at each measurement pressure was less than 0.4 kPa, relatively $4\times10^{-6}$ of the maximum pressure. The measurement repeatability of the pressure transducer when it was calibrated in the hydraulic pressure calibration system was almost same with that when it was calibrated in the developed gas pressure calibration system.

The difference between the calibration values of the pressure transducer using gas and liquid media, $D_{gas}$ and $D_{liq}$, in ascending processes is shown in Fig. 2.9. Error bars indicate standard uncertainties of the calibration results in the developed gas pressure calibration system. The differences were sufficiently smaller than the error bars. Therefore, the calibration values by the developed gas pressure calibration system was consistent with the values by hydraulic pressure calibration systems at pressures up to 100 MPa. The validity of the developed calibration system was confirmed.
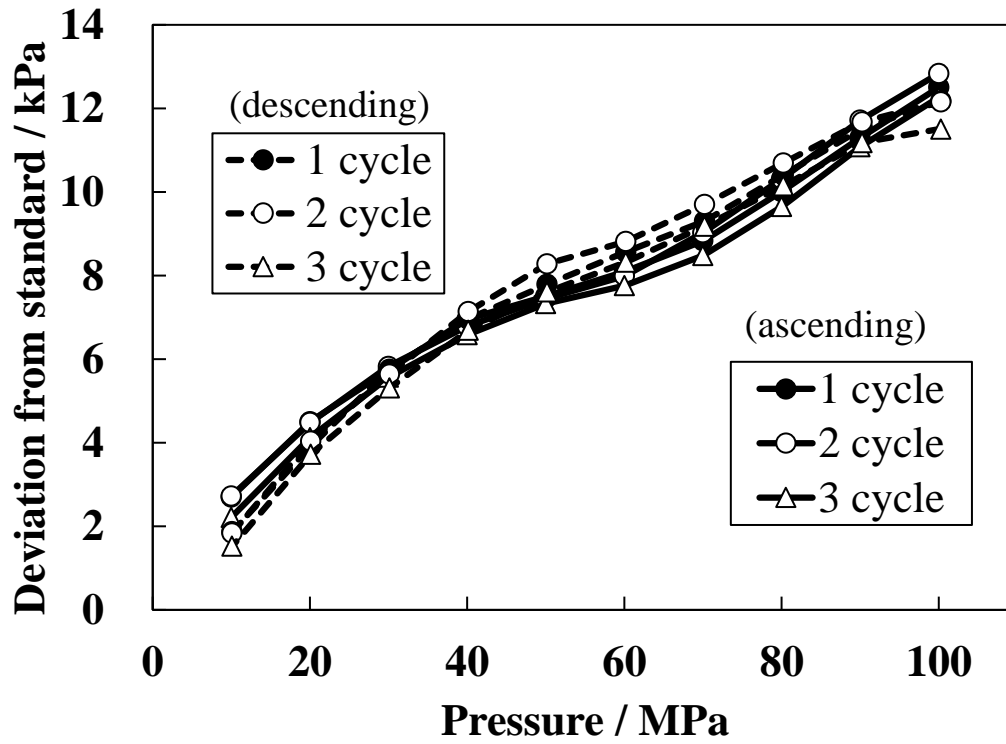
Figure 2.8. Calibration result of a pressure transducer by the existing hydraulic pressure calibration system. Solid line shows ascending process and dashed line shows descending process. The results of three calibration cycles are shown separately.
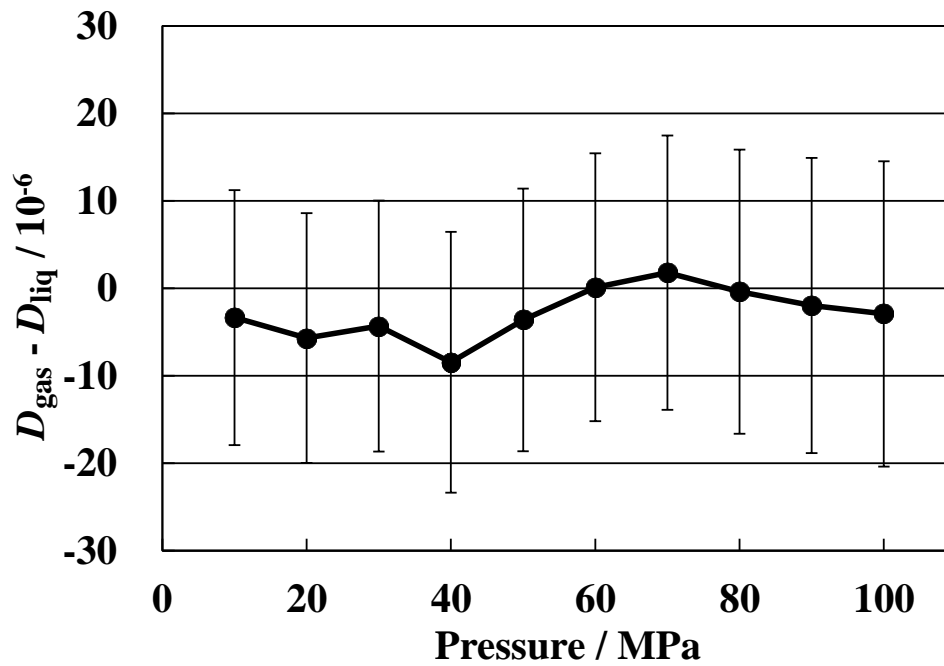


Figure 2.9. Differences between the calibration results by the developed gas pressure calibration system and that by the existing hydraulic pressure calibration system.

## 2.4.2 International comparison

To ensuring international equivalence of measurement standard, an international comparison was conducted. International comparisons are also important for strengthening the international competitiveness of industry. The objective of the comparison was to compare the performance of gas pressure standards in the pressure range 10 MPa to 100 MPa. The comparison was a bilateral comparison between National Metrology Institute of Japan, AIST (NMIJ, Japan) and National Institute of Standards and Technology (NIST, the United States). This is the world's first international comparison for gas pressure standard of high-pressure range. Only the United States and Germany have capabilities of the gas pressure calibration up to 100 MPa [6, 7]. The comparison is identified as APMP.M.P-S6 [21] by the Consultative Committee for Mass and Related Quantities (CCM) of the International Committee for Weights and Measures (CIPM), and the Asia-Pacific Metrology Programme (APMP).

The transfer standard was prepared which mainly consists of two high precision pressure transducers, shut-off valves and an environment monitoring device. Two pressure transducers are used as the transfer standard to provide redundancy and ensure reliability. Table 2.2 shows the information of selected pressure transducers used as the transfer standard. Both pressure transducers are quartz Bourdon-type. The transfer standard was calibrated by each institute, and the calibrated values were compared. The pressure transducers were characterized beforehand, e.g. the data scattering, the repeatability, the long-term stability, the temperature dependency, and the effect of gas type, for value correction and uncertainty evaluation. Nitrogen was used in NMIJ and helium was used in NIST as the pressure medium. The standard device of NIST is different type with our standard device [7]. NIST uses helium due to the specifications of standard device. Evaluation of the effect of gas type is described detail in section 3. The comparison results showed in Fig. 2.10. Error bars indicate expanded uncertainties ($k = 2$). The degrees of equivalence between the two institutes were evaluated by the relative differences of the participant's results and their associated combined expanded uncertainties ($k = 2$). All of the results showed agreements within their expanded uncertainties ($k = 2$). Internal equivalence of the developed gas pressure standard for pressures up to 100 MPa was ensured by the international comparison.

Table 2.2. Pressure transducers used as the transfer standard.

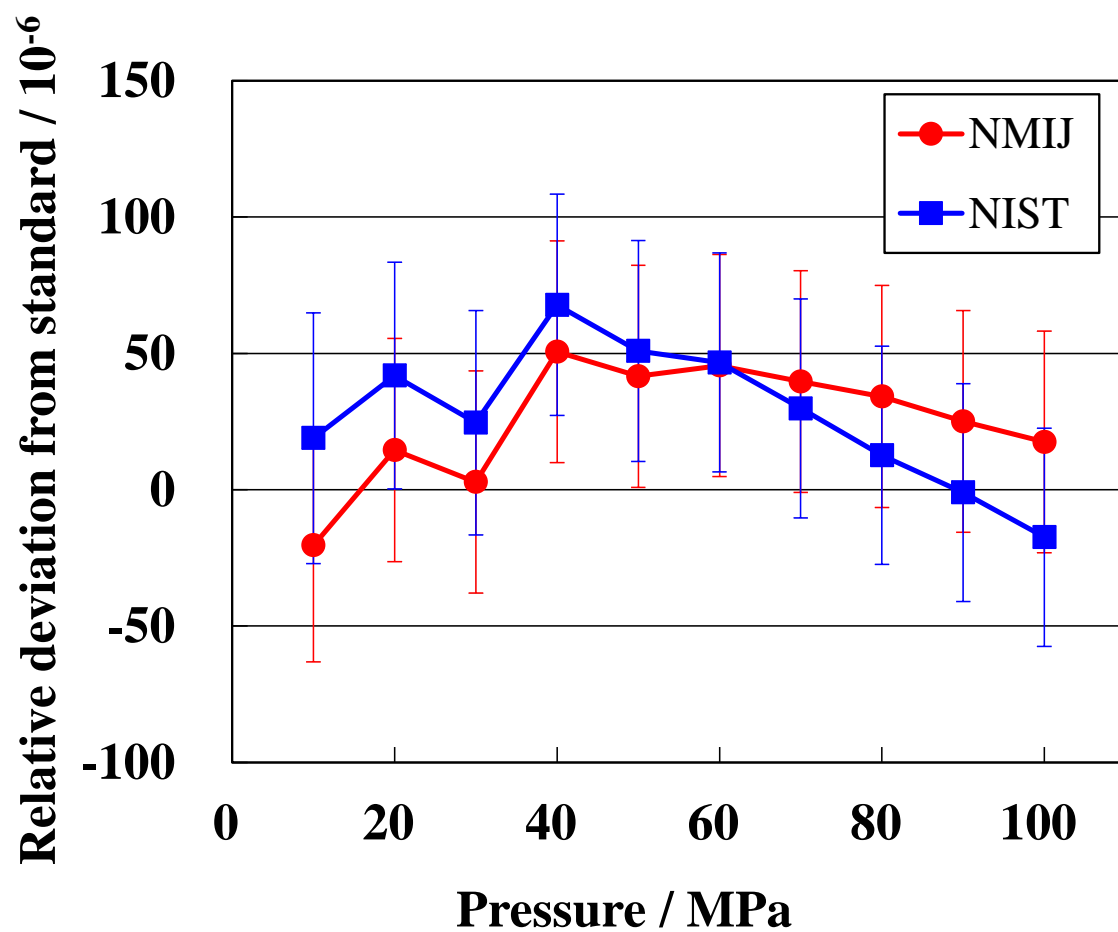| Manufacturer | Fluke calibration | Paroscientific, Inc. |
|---|---|---|
| Model | RPM4 A100Ms | 745-15K |
| Sensor | Quartz reference pressure transducer | Digiquartz® Transducer |
| Pressure range | 100 MPa | 103 MPa (15,000 psi) |
| Resolution | 0.0001 % | 0.0001 % |
| Normal operating temperature range | 15 ℃ - 35 ℃ | 0 ℃ - 40 ℃ |

Figure 2.10.   Results of international comparison between NMIJ (Japan) and NIST (The United States). All of the results show agreements within their uncertainties.

## 2.5  Characterization of calibration system

## 2.5.1  Fall rate of liquid-lubricated piston-cylinder

In this section, the characteristics of the developed calibration system were evaluated. The piston falls at a specific speed owing to the leakage of the pressure medium through the gap between the piston and cylinder. The fall rate of the piston is an important characteristic for operating pressure balances. The fall rate of the piston is an indicator for checking the operation of the pressure balance and the leakage of the calibration system. The fall rate of a liquid-lubricated piston-cylinder might depends on the pressure medium. The effect of pressure medium on the fall rate of the liquid-lubricated piston-cylinder is discussed here. The fall rate of the liquid-lubricated piston-cylinder when gas pressure is generated is compared with that when hydraulic pressure is generated. The fall rate was measured by the following method. In the stepwise calibration cycles, after the piston position was adjusted to an appropriate position, the shut-off valve shown in Fig. 2.1 was closed, and the pressure balance and the pressure transducer were separated from the pressure control system. When the output of the device under calibration was sampled in the calibration, the piston position is also sampled. The fall rate was calculated from 18 piston positions at 10 sec intervals after waiting seven minutes at each pressure. The fall rate is calculated by the change of the piston position over time.

Fig. 2.11 shows the fall rate of the liquid-lubricated piston-cylinder when hydraulic pressure is generated. In the figure, solid lines show the ascending process and dashed lines show the descending process. The fall rates of three cycles are shown separately. Fall rates does not change depending on the process. The fall rate increased with pressure at low pressure (less than 40 MPa), and decreased with pressure at high pressure (more than 40 MPa). If the clearance of the piston-cylinder is not changed by the generated pressure, the fall rate would increase constantly with generated pressure due to increased leakage of the pressure medium. However, the clearance of the liquid-lubricated piston-cylinder narrows with pressure, because the liquid-lubricated piston-cylinder is a re-entrant type, and the fall rate decreases with pressure at high pressure range, as shown in Fig. 2.11.
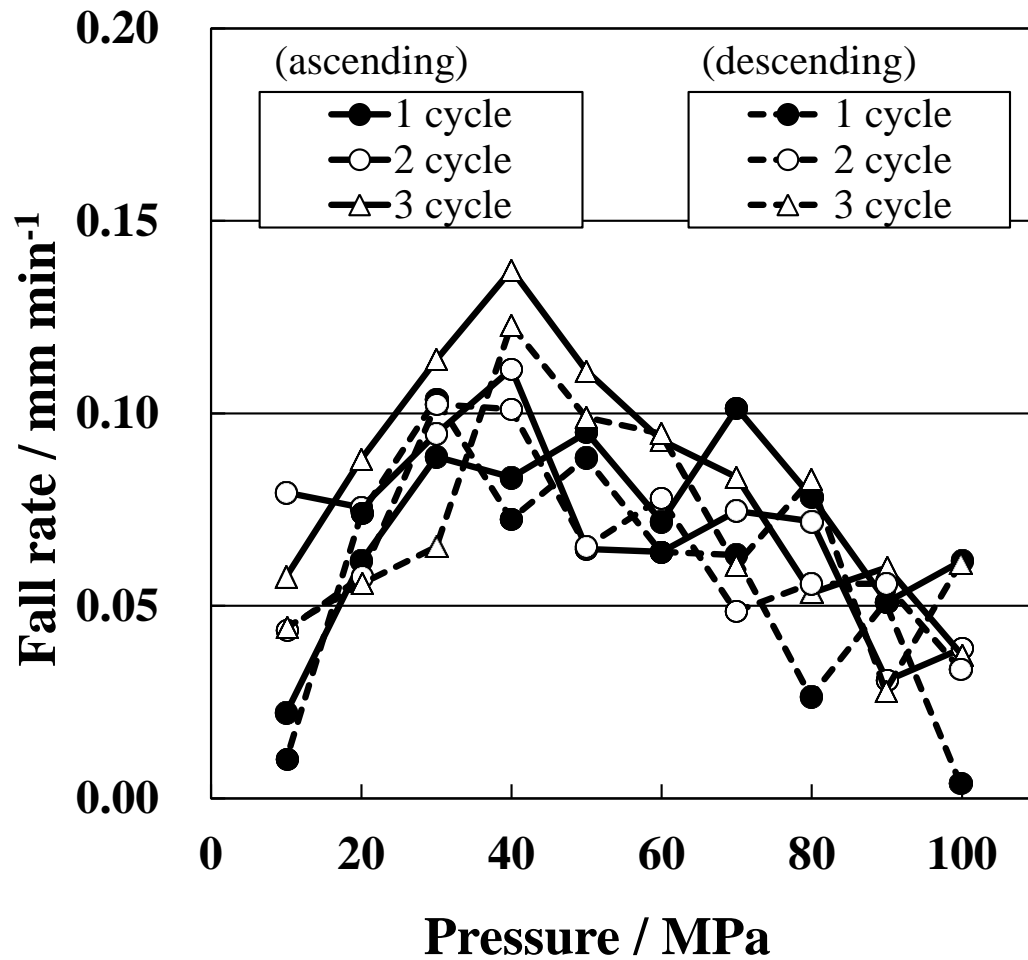
Figure 2.11. Pressure dependence of fall rate of a liquid-lubricated piston-cylinder when hydraulic pressure is generated.

Fig. 2.12 shows the fall rate of the liquid-lubricated piston-cylinder when gas pressure is generated. The fall rates obtained from three stepwise cycles are plotted. Solid lines show the ascending process and dashed lines show the descending process. There was a clear difference between the fall rates in the ascending process and that in the descending process. When gas pressure is generated, a gas-liquid boundary plane exists in the reservoir of the liquid-lubricated piston-cylinder. It is thought that the fall rate changes because the gas dissolves into the liquid. The mass of gas dissolved into the liquid is proportional to the pressure, following Henry's law. This gas dissolution has different effect on the fall rate in the ascending process and that in the descending process. The gas volume is reduced in the ascending process due to the dissolution into the liquid, increasing the piston fall rate as compared to that when hydraulic pressure is generated. In the descending process, dissolved gas escaping from the liquid and the gas volume conversely increases. The piston fall rate in the descending process is thus smaller than that in the ascending process, and the piston rises at below 30 MPa.
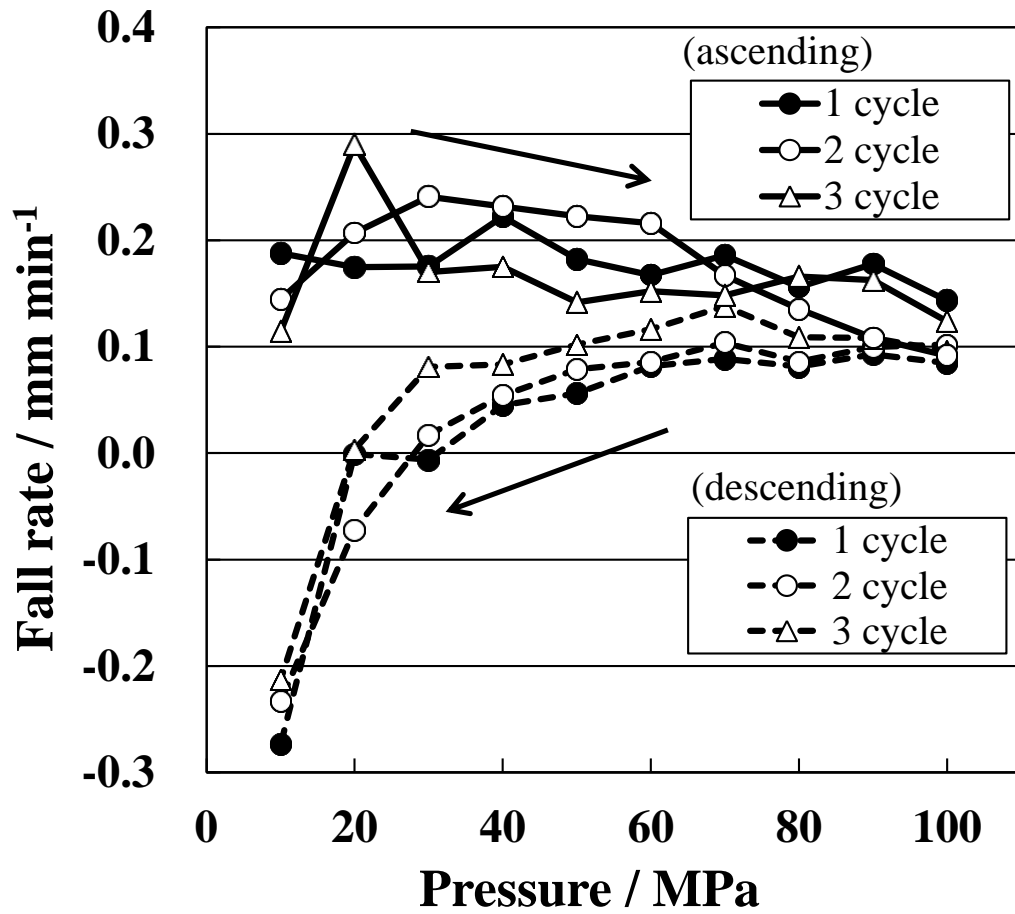
19

Figure 2.12. Pressure dependence of fall rate of a liquid-lubricated piston-cylinder when gas pressure is generated. There is a clear difference between the fall rates in ascending and descending processes

When the fall rate was measured in Fig. 2.12, it was thought that the gas dissolution was not reached the equilibrium state. Therefore, the time change of the fall rate after the pressure reaches at 10 MPa is investigated. The change of fall rate was measured by continuously generating a constant pressure in the ascending and descending processes. The fall rate at each elapsed time were measured after the piston position is adjusted to the appropriate position. Fig. 2.13 shows the time change of the fall rate of the liquid-lubricated piston-cylinder after the pressure reaches at 10 MPa in the ascending and descending processes. The horizontal axis shows elapsed time after the gas pressure roughly stabilized at 10 MPa. In the figure, solid circles indicate the fall rate in the ascending process, and open circles indicate that in the descending process. The dashed line shows the fall rate of the same piston-cylinder when hydraulic pressure is generated. The fall rate of the piston generating the hydraulic pressure does not change with elapsed time. In the ascending process, the fall rate of the piston generating the gas pressure decreased with elapsed time, and reached the fall rate of the piston generating the hydraulic pressure after two hours. The fall rate after that was almost constant because the gas dissolution into the liquid reached a nearly equilibrium state. In contrast, the fall rate in the descending process increased with elapsed time . This

change was the opposite direction compared with the ascending process. The fall rate reached the fall rate of the piston generating the hydraulic pressure after two hours because the outgassing from the liquid reached a nearly equilibrium state.

The difference between the fall rate of the liquid-lubricated piston-cylinder generating the gas pressure and the hydraulic pressure can be thus explained by the gas dissolution into the liquid at the gas–liquid boundary plane of the liquid-lubricated piston-cylinder. Because the piston fall rate significantly changes with elapsed time as described, the liquid-lubricated pressure balance needs to be operated with care.
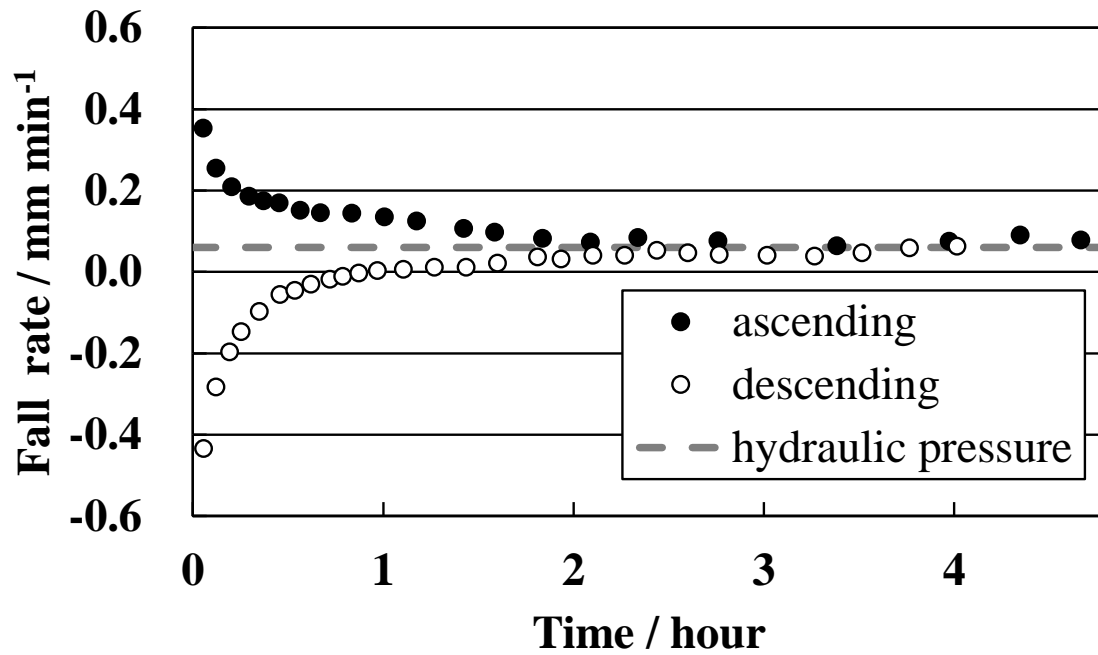


Figure 2.13. Change of fall rate with elapsed time after pressure reaches at 10 MPa. The gas dissolution reached equilibrium state two hours after the pressure reaches at 10 MPa in both ascending and descending processes.

## 2.5.2  Measurement of gas temperature in piping

High-pressure gas system compresses and expands gas due to the pressure change and should consider the change of gas temperature. When gas is rapidly compresses or expands due to the pressure change, its temperature greatly changes by an adiabatic process. In the developed calibration system, if the temperature of gas in the piping greatly changes during data sampling in the calibration, the stability of the generating pressure may be affected.

To evaluate the change of gas temperature during calibration cycles, a sheathed thermocouple, manufactured by Okazaki Manufacturing Company (T35-SP, type T), with 0.5 mm diameter was inserted into the pressure piping in the developed calibration system. The resolution of the thermocouple is 0.1 °C. Custom-made fittings were attached to the thermocouple for insertion into the high-pressure piping.

It can be predicted that a large pressure change will cause a temperature change due to the adiabatic process. Changes in temperature measured by the thermocouple and pressure over time during a stepwise calibration cycle is shown in Fig. 2.14. The temperature in the pressure piping gradually decreased from 24.0 °C to 23.5 °C according to changes in the environmental temperature. When measurement pressure point was changed to the next point, the pressure rapidly changed and abrupt temperature changes were observed. In the ascending process, nitrogen was compressed, and the temperature rapidly rose. In descending process, nitrogen was expanded, and the temperature rapidly dropped.

For focusing on the moment of pressure change, Fig. 2.15 shows the temperature change when the gas pressure changes from 0 MPa to 10 MPa. The temperature first rapidly rose from 24.0 °C to 26.3 °C immediately after the start of pressurization. Then the temperature exponentially dropped when the pressurization speed became slow. Thereafter, the temperature returns to the initial value when the pressurization is completed.

The calculated temperature change assuming ideal adiabatic compression is much larger than the observed temperature change of 2.3 °C. Since it took more than a minute to change the pressure from 0 MPa to 10 MPa in the developed calibration system, the heat exchange between the gas and the metal piping was occurred. The gas temperature returned to the initial temperature because of the heat exchange. Therefore, the compression and the expansion of gas in the developed calibration system is not ideal adiabatic compression.

The changed temperature of gas returned its initial value within a few minutes after the pressure change. Since the calibration data is sampled at least seven minutes after the pressure change, the temperature during data sampling in the calibration was sufficiently stable. Therefore, the effects of temperature change on the calibration can be negligible in the developed calibration system.
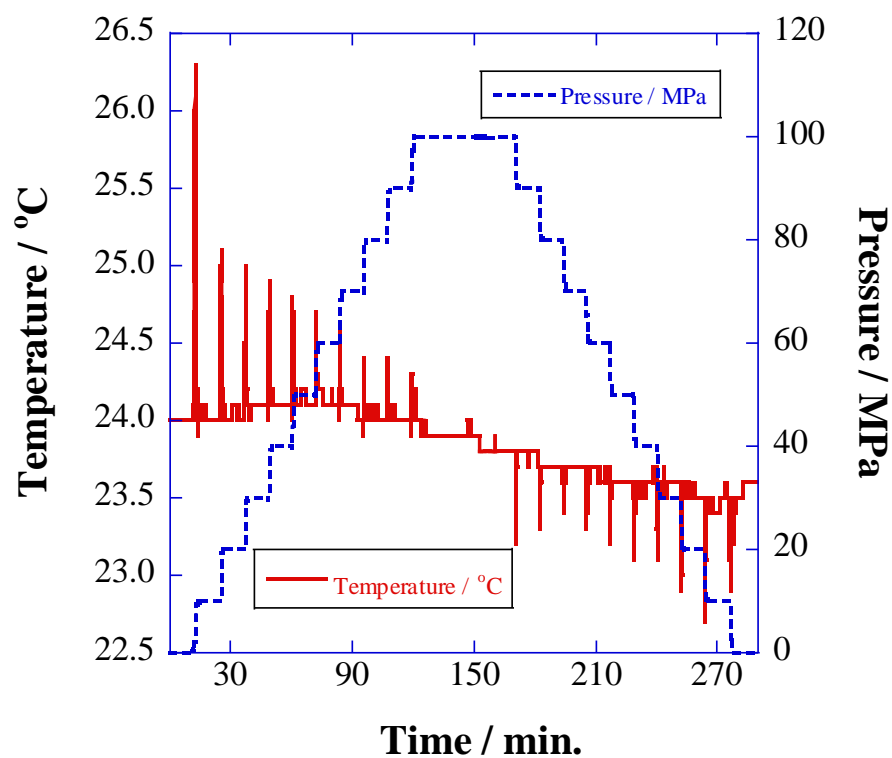
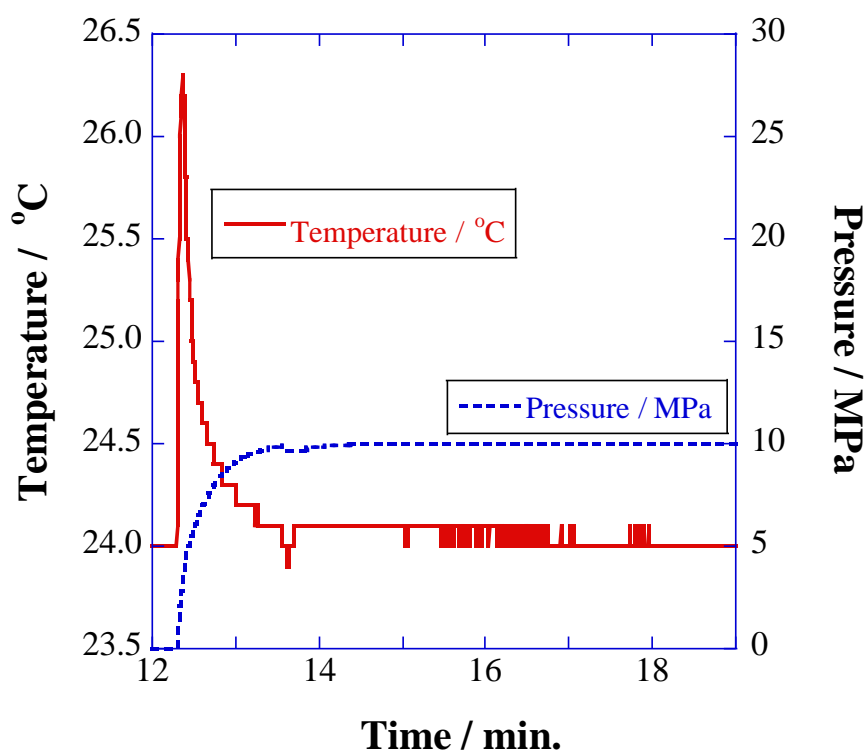Figure 2.14. Gas temperature and pressure during a stepwise calibration cycle.



Figure 2.15. Change of temperature and pressure with elapsed time when pressure changes from 0 MPa to 10 MPa.

# 3. Effects of type of gas on calibration values of pressure transducers

## 3.1 Consideration about the effect of type of gas

To perform precision pressure measurements, it is necessary to periodically calibrate the pressure gauges and understand their characteristics. Detailed characterization of pressure gauges of ultra high-pressure gas had not been performed because there was no measurement standard. The calibration value of pressure gauges might be affected by the type of gas used. Since the pressure transducers are used for various applications and measure the pressure of various gas, the effect of the type of gas on the calibration values is important characteristics. In the international comparison, we have found that the quartz Bourdon-type pressure transducers [15 - 17] are affected by the type of gas used. There was different between the calibration value of the pressure transducer when nitrogen was used as the pressure medium and that when helium was used. The trend and amount of the effect was different for the two transducers. The reason for the effect has not been clarified yet. In case that measuring gas is different from gas used in the calibration, precision pressure measurement cannot be performed due to the effect. To realize precision pressure measurement of ultra high-pressure gas, it is necessary to find the reason for the effect of the type of gas, and investigate the correction method and the reduction method of the effect. To understand characteristics of the quartz Bourdon-type pressure transducers, the effect of the type of gas on the calibration values was evaluated in detail with developed calibration system.

The reason for the effect is examined with a focus on the gas density and the structure of the sensing element of the pressure transducer. The sensing element of the quartz Bourdon-type pressure transducer mainly consists of a Bourdon tube and a quartz crystal oscillator. Bourdon tubes are commonly used as pressure gauges [42]. The quartz crystal oscillator is attached to the Bourdon tube as shown in Fig. 3.1. A pressure applied to the Bourdon tube generates an uncoiling force that applies tension to the quartz crystal. The change in frequency of the quartz crystal oscillator as a function of tension is a measure of the applied pressure. A normal Bourdon-type pressure gauge has low accuracy, but the quartz Bourdon-type pressure transducer achieves high resolution and high accuracy by using the quartz crystal oscillator. The accuracy of the pressure transducers is about 0.01 % of full scale and the resolution of them is less than $1 \times 10^{-6}$ of full scale. The pressure transducer is used for precision high-pressure measurements. It was thought that there would be no effect from the type of gas because the measuring gas does not directly contact the quartz crystal in the sensing element. By evaluating with the developed calibration system, we were able to find the effect for the first time.
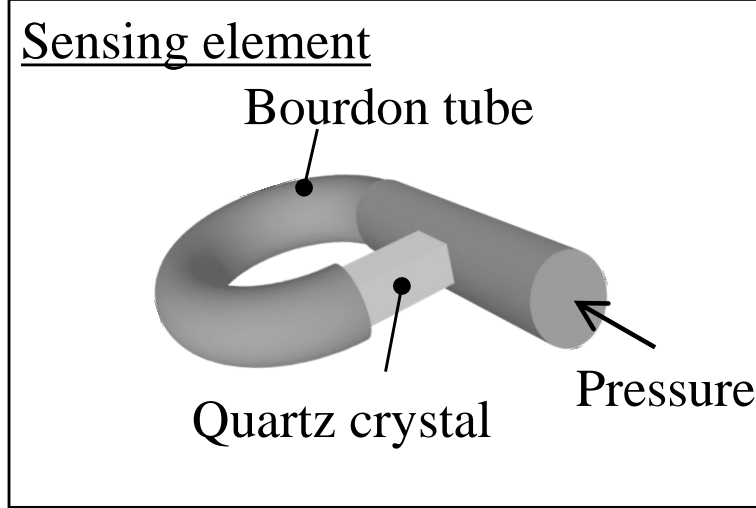
Figure 3.1. Schematic drawing of sensing element of a quartz Bourdon-type pressure transducer. Applied pressure generates an uncoiling force in Bourdon tube.

In this study, we postulate that the weight of the measuring gas inside the Bourdon tube affect the indication of the pressure transducer. The density of gas at high pressure is hundreds of times larger than the density at atmospheric pressure. The weight of the gas can cause extensional or compressional deformation of the Bourdon tube by gravitational force in addition to the deformation due to the applied pressure. Therefore, the oscillating frequency of the quartz crystal is changed and hence the indication of the pressure transducer is affected. In this case, the indication can be expressed as the sum of two contributions. First term is the force acting on the Bourdon tube purely from the applied pressure and second term is the extensional or compressional gravitational force from the weight of gas inside the Bourdon tube. The second term depends on the weight (density) of gas. Since the gas density largely differs depending on the type of gas, the indications of the pressure transducers can be significantly affected by the type of gas. The second term also depends on the relation between the directions of the gravitational force and the deformation of the Bourdon tube. For example, when the gravitational force and the deformation of the Bourdon tube are in the same direction, the weight of gas occurs the extensional deformation of the Bourdon tube and the indication increases. On the other hand, when the gravitational force and the deformation of the Bourdon tube are in the opposite direction, the weight of gas occurs the compressional deformation and the indication decreases.

When the pressure transducer and the Bourdon tube inside the pressure transducer are oriented horizontally, as shown in Fig. 3.2 (a). The relation between the directions of gravitational force and the deformation of the Bourdon tube depends on the rotation angle $\theta$ of the pressure transducer. Then, the second term depends on the relation and can be expressed using a sinusoidal curve against the rotation angle. When the pressure transducer is oriented horizontally, the indication of the pressure transducer with the rotation angle $\theta$, $I_{p,\theta}$, is expressed by the following equation.

25

$$I_{p,\theta} = I_{p,\theta_0} + \Delta I_{p,\mathrm{h}} \times \sin(\theta - \theta_0). \qquad (3.1)$$

Here, the first term $I_{p,\theta_0}$ represents the contribution purely from the applied pressure, and $\Delta I_{p,\mathrm{h}}$ represents the effect of the weight of the measuring gas inside the Bourdon tube when the pressure transducer is oriented horizontally. The parameter $\theta_0$ is the angle at which the indication $I_{p,\theta}$ is not affected by the weight of gas, where $I_{p,\theta}$ becomes equal to $I_{p,\theta_0}$. When the pressure transducer is oriented at rotation angle $\theta_0$, the indication of the transducer is expected to be not affected by the type of gas.

When the pressure transducer is oriented vertically, as shown in Fig. 3.2 (b), it is thought the indication of the pressure transducer at upward and downward orientations, $I_p$, is expressed by the following equation.

$$I_p = I'_p \pm \Delta I_p. \qquad (3.2)$$

Here, the first term $I'_p$ represents the contribution purely from the applied pressure, and $\Delta I_p$ represents the effect of the weights of the measuring gas inside the Bourdon tube when the transducer is oriented vertically. $\Delta I_p$ depends on both the type of gas and the orientation of the transducer. The sign of $\Delta I_p$ depends on the relation between the directions of the gravitational force and the deformation of the Bourdon tube. When the transducer is oriented upward, the sign of $\Delta I_p$ is negative because the gravitational force arising from the weight of gas causes compressional deformation of the Bourdon tube. Conversely, when the transducer is oriented downward, the sign of $\Delta I_p$ is positive because the gravitational force causes extensional deformation.

The above assumption is experimentally confirmed by calibrating the pressure transducer at different orientations in section 3.2. If the indication of the pressure transducer is affected by the weight of the gas, the calibration value should depend on the orientation of the pressure transducer.

We also hypothesized that the level of variation by the type of gas may be correlated with the density of the measuring gas in the Bourdon tube. In section 3.3, we evaluate the relationship between the level of variation and the density of gas in detail, using a total of six different gas densities.
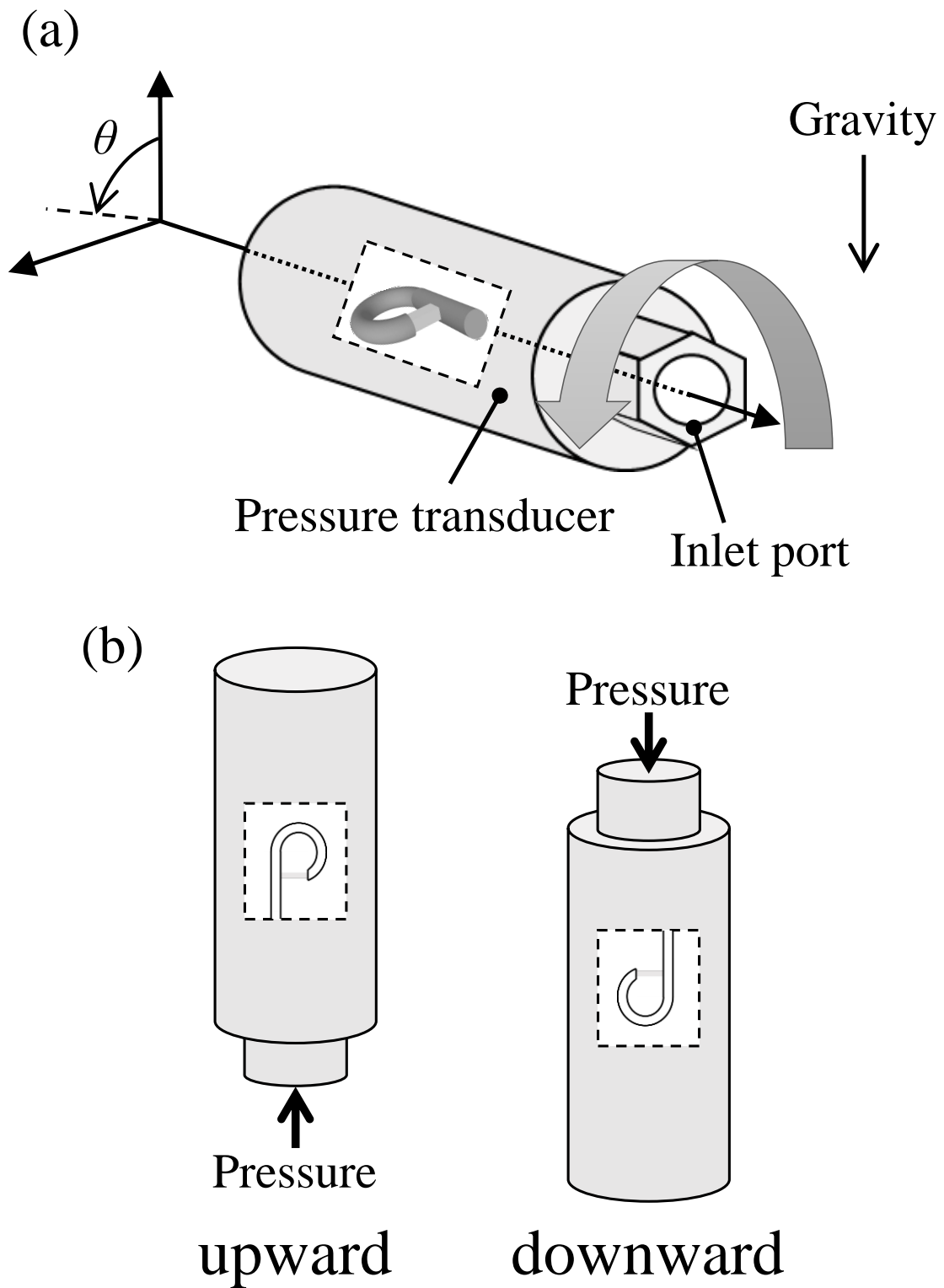
Figure 3.2. Orientation of quartz Bourdon-type pressure transducer. (a) Pressure transducer is oriented horizontally. (b) Pressure transducer is oriented vertically.

## 3.2 Evaluation of effect of orientation

### 3.2.1 Evaluation method

If the indication of the pressure transducer is affected by the weight of the gas, the calibration value should depend on the orientation of the pressure transducer. To evaluate the effect of the orientation of the pressure transducer on the calibration value, the quartz Bourdon-type pressure transducers, manufactured by Paroscientific, Inc. (Model 9000-15K, pressure range 100 MPa), [15] were calibrated by using the developed calibration system. The calibration was performed by applying the same pressure to the liquid-lubricated pressure balance used as the standard device and the pressure transducer. The pressure transducer was calibrated by comparing the indication of the pressure transducer with the value of the standard device. Two quartz Bourdon-type pressure transducers A and B were calibrated simultaneously. The measurement pressure was from 0 MPa to 100 MPa at every 10 MPa. After the calibration cycle was completed, the orientation of the pressure transducer was changed to the next.

The difference between the indication of the pressure transducer and the pressure applied by the standard device after offset correction, $R_p$, is calculated as

$$R_p = (I_p - S_p) - (I_0 - S_0). \qquad (3.3)$$

Here, $I_p$ is the indication of the pressure transducer. $S_p$ is the pressure applied by the standard device. The subscript 0 means the value when the atmospheric pressure is applied. The mean value of $R_p$ in three ascending processes is used as the calibration value. The calibration values of the pressure transducer at each orientation are compared.

### 3.2.2 Calibration values at different orientation

First, the results of horizontal orientation are shown. The horizontally oriented pressure transducers as shown in Fig. 3.2 (a), were calibrated at four rotation angles: 0°, 90°, 180°, and 270° from the initial setting condition. The rotation angle 0° is not related with the direction of the Bourdon tube inside the pressure transducer because it is impossible to identify the direction from the transducer's outer appearance. Nitrogen was used as pressure medium.

The calibration value at rotation angle $\theta$, $R_{p,\theta}$, is expressed by the following equation from Eqs. (3.1) and (3.3).

$$R_{p,\theta} = R_{p,\theta_0} + \left(\Delta I_{p,\text{h}} - \Delta I_{0,\text{h}}\right) \times \sin(\theta - \theta_0). \qquad (3.4)$$

Here, $R_{p,\theta_0} = (I_{p,\theta_0} - S_p) - (I_{0,\theta_0} - S_0)$. $R_{p,\theta_0}$ is the calibration value when the rotation angle is $\theta_0$.

28

The density of nitrogen [43] changes greatly with pressure. In this study, the target pressure is more than 10 MPa. The density of nitrogen at 10 MPa is about one hundred times larger than that at atmospheric pressure. We hypothesized that $\Delta I_{p,\text{h}}$ is correlated with the density of the gas. Therefore, $\Delta I_{0,\text{h}}$ was less than one one-hundredth of $\Delta I_{p,\text{h}}$ and was negligibly small. Eq. (3.4) is changed to

$$R_{p,\theta} = R_{p,\theta_0} + \Delta I_{p,\text{h}} \times \sin(\theta - \theta_0). \qquad (3.5)$$

Fig. 3.3 shows the calibration results of the pressure transducers at the four rotation angles: 0°, 90°, 180°, and 270°. Error bars indicate the standard deviation of $R_{p,\theta}$ obtained from three ascending processes. In both pressure transducers, $R_{p,\theta}$ clearly depended on the rotation angle at all pressures. The difference in calibration value depending on the rotation angle differed depending on the pressure transducer.
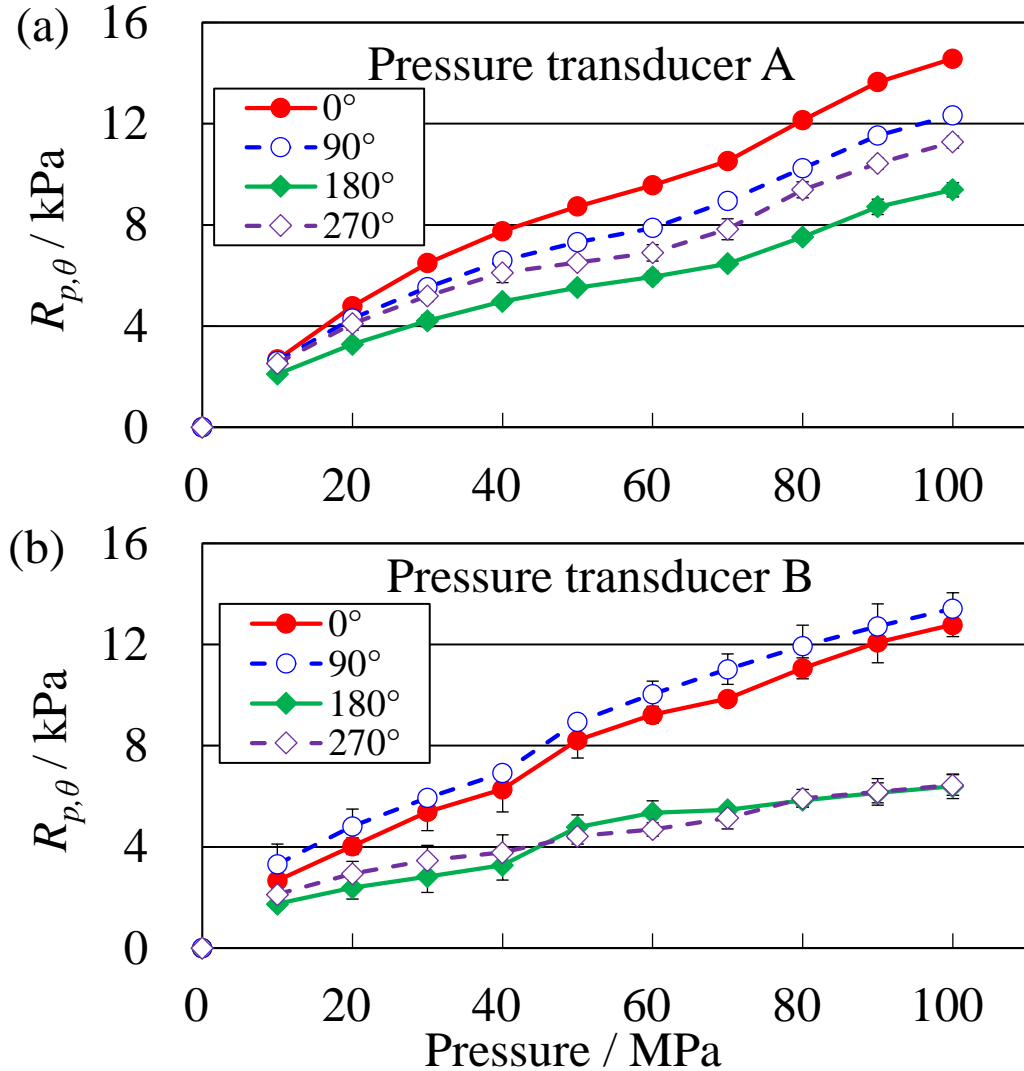


Figure 3.3. Calibration values $R_{p,\theta}$ at four rotation angles ($\theta$ = 0°, 90°, 180°, and 270°): (a) pressure transducer A and (b) pressure transducer B. Calibration values depended on the rotation angle in both pressure transducer.

The dependence on the rotation angle is examined in detail. Fig. 3.4 shows the dependence on the rotation angle $\theta$ of the calibration value $R_{p,\theta}$ at 100 MPa. $R_{p,\theta}$ is fitted with a sinusoidal function. The coefficients, $R_{p,\theta_0}$, $\Delta I_{p,h}$, and $\theta_0$ in Eq. (3.5) were obtained by fitting. The obtained coefficients are shown in Fig. 3.5. The errors of $R_{p,\theta_0}$ and $\Delta I_{p,h}$ were less than 0.3 kPa and 0.4 kPa, respectively. The error of $\theta_0$ was less than 10° at pressures above 20 MPa. $\theta_0$ at low pressure had large error because $\Delta I_{p,h}$ at low pressure was small and the fitting was difficult. Although $R_{p,\theta_0}$ and $\Delta I_{p,h}$ was changed by pressure, $\theta_0$ was almost constant in all pressure because $\theta_0$ was determined by only the relationship between the directions of the gravitational force and the deformation of the Bourdon tube. The average values of $\theta_0$ in pressure transducers A and B were about 280° and 320°, respectively. When the pressure transducer is oriented at rotation angle $\theta_0$, the indication of the transducer is expected to be not affected by the type of gas. $\Delta I_{p,h}$ depend on the pressure transducer, and it means the level of variation depend on the pressure transducer. $\Delta I_{p,h}$ of pressure transducer A and B at 100 MPa are 2.7 kPa, and 4.7 kPa, respectively.
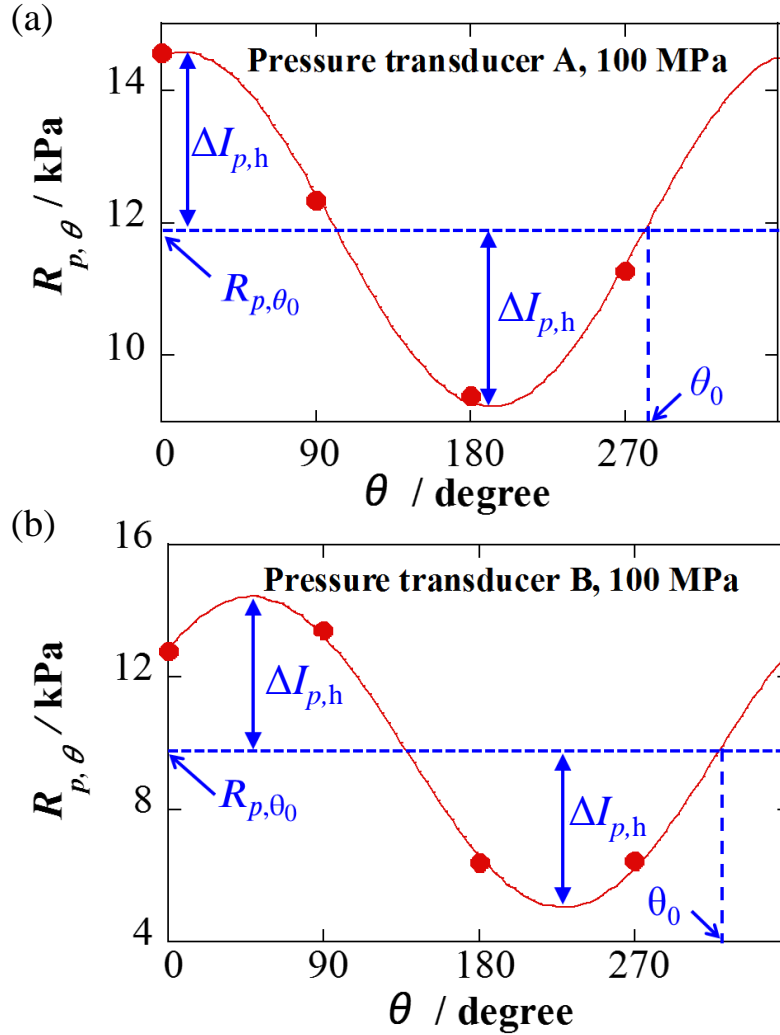


Figure 3.4. Calibration values $R_{p,\theta}$ of (a) pressure transducer A and (b) pressure transducer B as a function of rotation angle $\theta$ at 100 MPa. Coefficients $R_{p,\theta_0}$, $\Delta I_{p,h}$, and $\theta_0$, in Eq. (3.5) are obtained by the fitting.
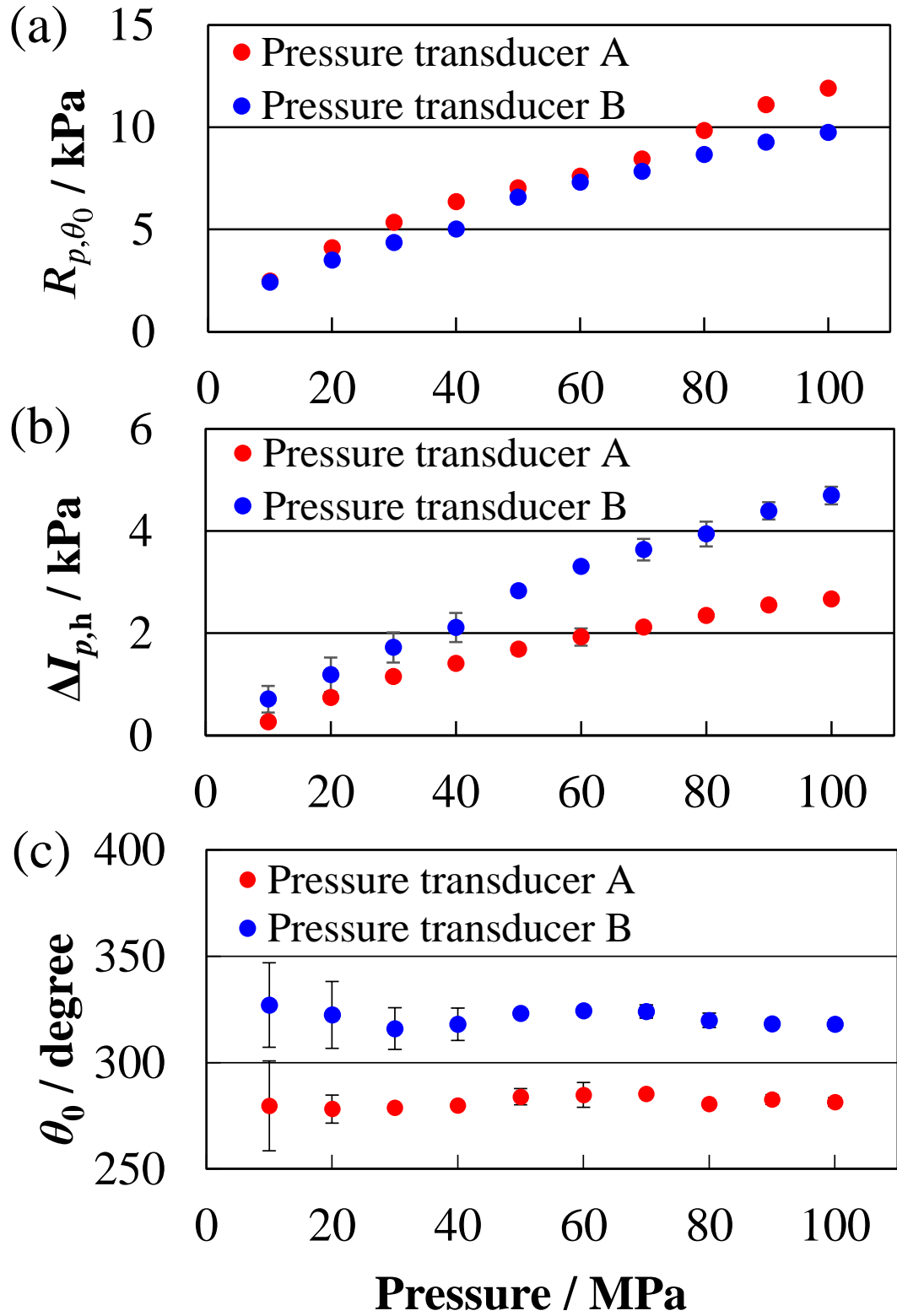
Figure 3.5. Coefficients (a) $R_{p,\theta_0}$, (b) $\Delta I_{p,\mathrm{h}}$, and (c) $\theta_0$, in Eq. (3.5) obtained from the dependence on the rotation angle of the calibration values.

Next, the results of vertical orientation are shown. When the pressure transduces are oriented vertically as shown in Fig. 3.2 (b), the calibration value, $R_p$, is expressed by the following equation from Eqs. (3.2) and (3.3).

$$R_p = R'_p \pm \Delta I_p. \qquad (3.6)$$

Here, $R'_p = (I'_p - S_p) - (I'_0 - S_0)$. $R'_p$ represents the contribution purely from the applied pressure, and is the calibration value not including the effect of weights of gas. $\Delta I_0$ was neglected because of the same reason with $\Delta I_{0,h}$ in Eq. (3.4). When the pressure transducer is oriented upward, the sign of $\Delta I_p$ is negative because the weight of gas occurs compressional deformation of the Bourdon tube. Conversely, when the pressure transducer is oriented downward, the sign of $\Delta I_p$ is positive because the weight of gas occurs extensional deformation.

The calibration values of the pressure transducers at the upward and downward orientations are shown in Fig. 3.6. Nitrogen and helium were used as pressure medium. The vertical axis shows the calibration value, $R_p$. $R_p$ depends on both the measuring gas and the orientation of the pressure transducer. The standard deviation of $R_p$ in three ascending processes was less than 0.6 kPa in all measurement pressure. The difference between $R_p$ at the upward and downward orientations was larger than the standard deviations. The difference at 100 MPa when nitrogen was used was about 7.0 kPa, relatively $7.0 \times 10^{-5}$ of full scale in pressure transducer A, and was about 10 kPa, relatively $1.0 \times 10^{-4}$ of full scale in pressure transducer B. The difference was comparable to the accuracy of the pressure transducer. When the transducer is oriented downward, the gravitational force arising from the weight of the pressure medium causes extensional deformation of the Bourdon tube, and when the transducer is oriented upward, the gravitational force causes compressional deformation. Therefore, $R_p$ at downward orientation was larger than $R_p$ at the upward orientation. The effects of the orientation with helium were smaller than that with nitrogen because the density of helium is smaller than that of nitrogen. The relationship between the effect and the density of gas is described in next section. At the same orientation, the maximum difference between $R_p$ with nitrogen and $R_p$ with helium was 3.3 kPa, relatively $3.3 \times 10^{-5}$ of full scale in pressure transducer A, and was 4.4 kPa, relatively $4.4 \times 10^{-5}$ of full scale in pressure transducer B.

The effect of the orientation is consistent with the assumption in section 3.1. The effects of the orientation and the type of gas could not be neglected for high precision measurement.
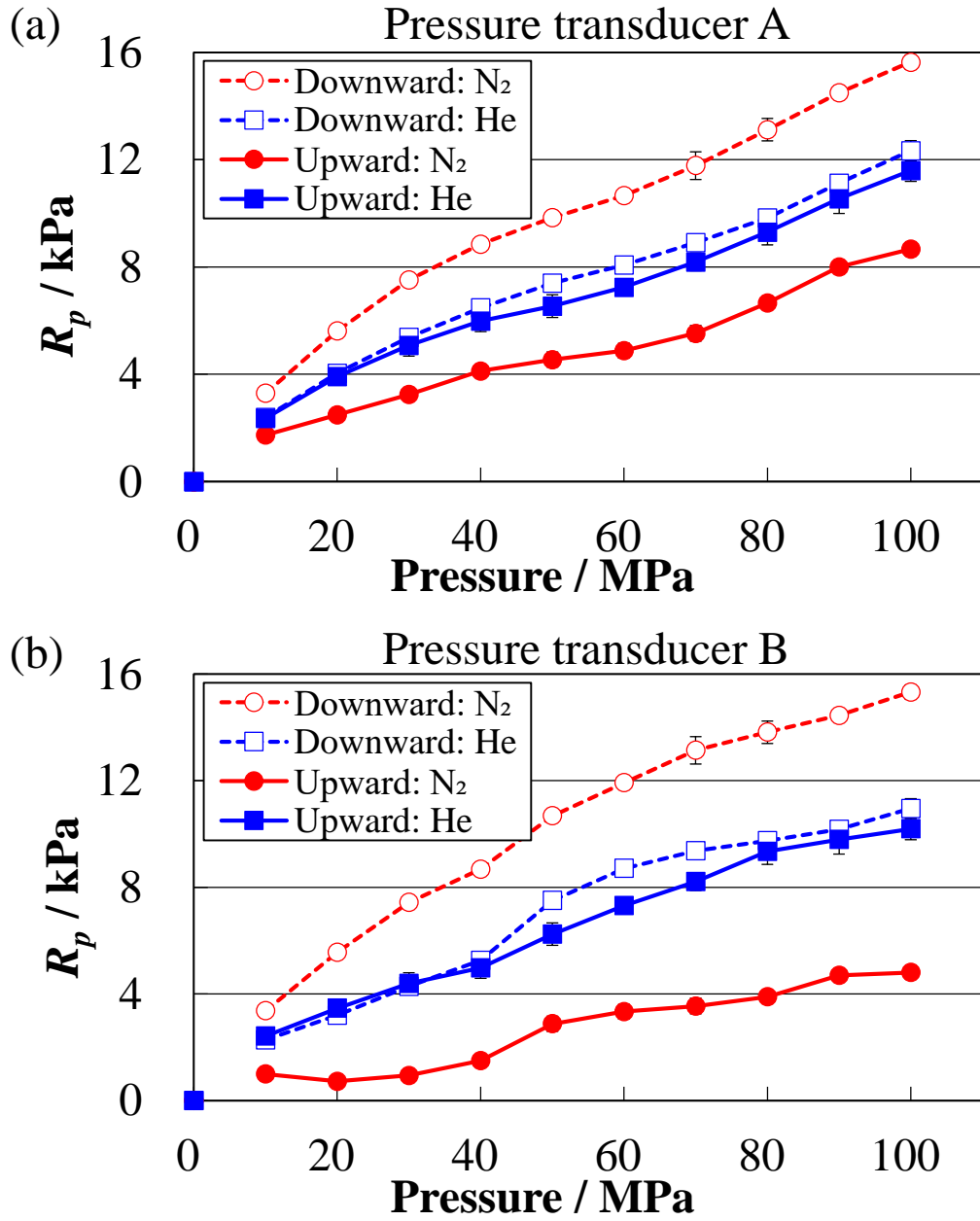
Figure 3.6. Calibration values $R_p$ of (a) pressure transducer A and (b) pressure transducer B at upward and downward orientations. Nitrogen and helium are used as pressure medium. Calibration values depend on both the measuring gas and the orientation of the pressure transducer.

## 3.3 Relationship between the effects of the pressure medium and density

### 3.3.1 Experimental setup

The level of variation due to the type of gas may be correlated with the density of gas in the Bourdon tube. In this section, we evaluate the relationship between the level of variation and the density of gas in detail, using a total of six different gas densities.

Fig. 3.7 shows the measurement system for both the level of variation and the density of ultra high-pressure gas. The measurement system is based on the developed calibration system. In this section, six gases with different densities (argon, nitrogen, helium, and three types of mixed gas) are used as the pressure medium. We prepared a separate gas cylinder for each pressure medium. The mixed gas is used to target densities between nitrogen and helium. The specific component ratios of the mixed gases are presented in Table 3.1. Although the component ratio was adjusted to within ± 0.4 % by a supplier, the ratio may change during the compression process in measurement system. Therefore, we measure the density of the gas in-situ at each measurement pressure.
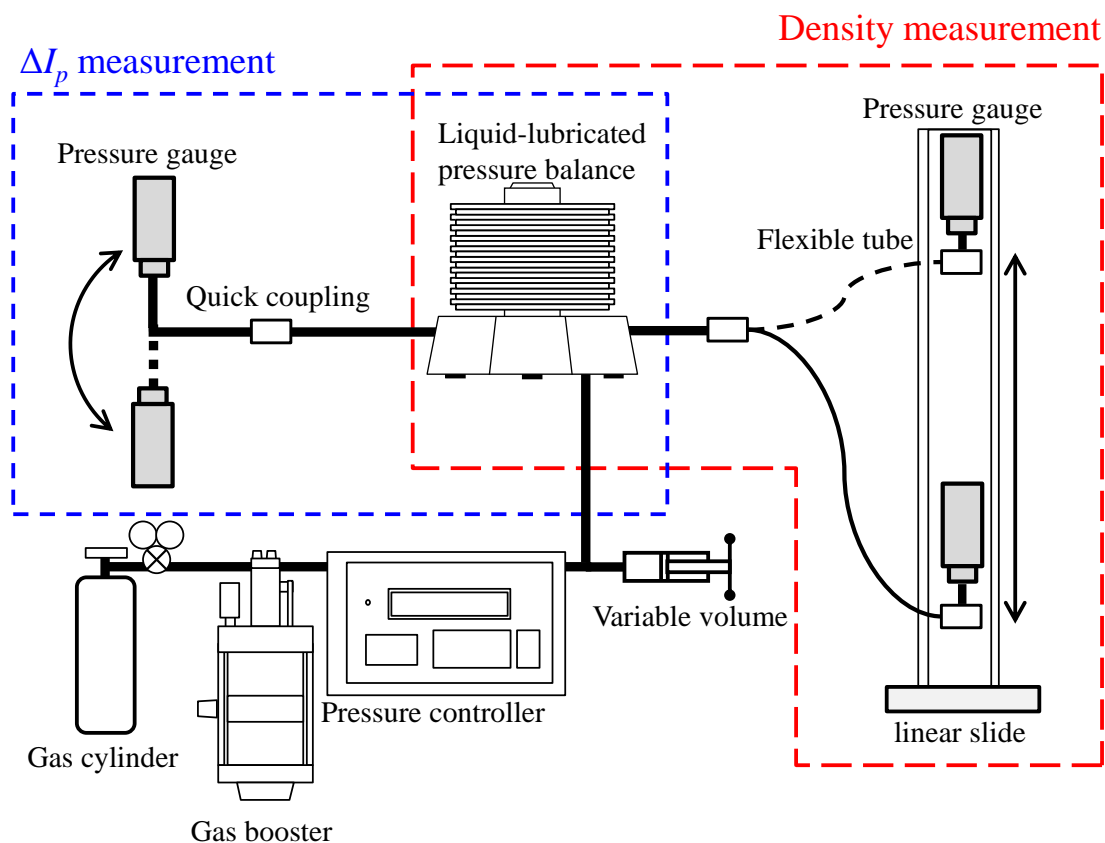


Figure 3.7. Measurement system for both the level of variation and the density of ultra high-pressure gas.

Table 3.1. Component ratios of mixed gases.

| Name | Ratio / % | |
| --- | --- | --- |
| | $N_2$ | He |
| $75N_2 25He$ | 75 | 25 |
| $50N_2 50He$ | 50 | 50 |
| $25N_2 75He$ | 25 | 75 |

To measure the level of variation in the calibration value due to changes in the pressure medium, $\Delta I_p$, a quartz Bourdon-type pressure transducer, manufactured by Paroscientific, Inc., (Model 9000-15K) is calibrated while oriented vertically upwards and downwards by the pressure balance. The orientation of the pressure transducer can be changed by loosening the quick coupling and rotating the pressure tube. The reference level of the transducer is set at a position of the internal Bourdon tube, separated from the inlet port by 116 mm.

To measure the density of the pressure medium in-situ, the pressure balance is also connected to another quartz Bourdon-type pressure transducer through a flexible tube. The pressure transducer is fixed on a sliding table of the linear slide, and then the vertical position of the pressure transducer can be changed while high pressure is applied. The maximum stroke of the linear slide is 2000 mm. The difference in pressure applied to the transducer due to the change in height position is accurately measured by the pressure balance [44, 45]. The density of the gas is then calculated from the differential pressure, the head difference, and the local gravity.

## 3.3.2 Effects of pressure medium on calibration values

As described in section 3.2, the calibration values are dependent on the orientation of the pressure transducers. When the transducer is oriented vertically, the effects of gravitational force is opposite for the upwards and downwards orientations. From Eq. (3.6), the level of variation in the calibration value due to changes in the pressure medium, $\Delta I_p$ is determined as half of the difference between the calibration values when oriented vertically upwards and downwards [20]. The pressure transducer was calibrated, in these orientations, from 10 MPa to 100 MPa at every 10 MPa step. Fig.3.8 shows the calibration results of the pressure transducer at the upward and downward orientations. The pressure medium was nitrogen. The average values of the calibration values at the upward and downward orientations are also shown. $\Delta I_p$ is the difference between the calibration values when oriented vertically upwards or downwards and its average value.
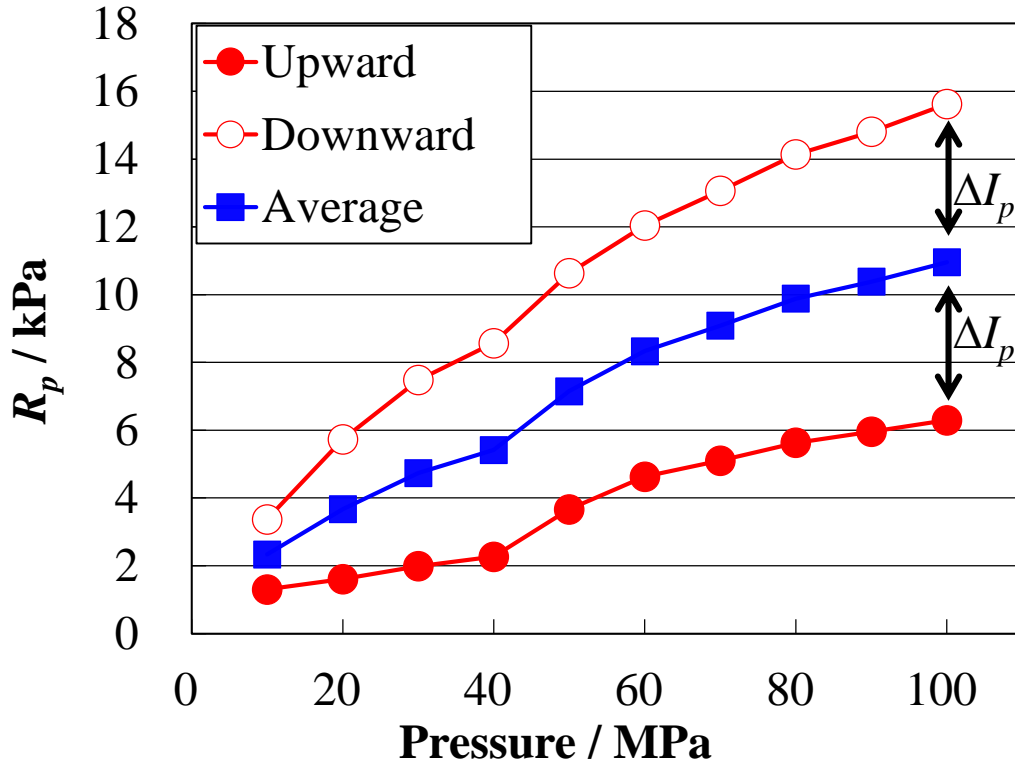
Figure 3.8. Calibration values of the pressure transducer at the upward and downward orientations and its average value. $\Delta I_p$ is determined as half of the difference between the calibration values when oriented vertically upwards and downwards

$\Delta I_p$ was evaluated using six gases, and the values are presented in Fig. 3.9. The error bars indicate the standard deviations of the $\Delta I_p$, calculated using the repeatability in the upward and downward orientations. From Fig. 3.9, it is clear that the value of $\Delta I_p$ is dependent on the type of gas as well as the pressure. $\Delta I_p$ increased as the pressure was increased, for each pressure medium. The largest $\Delta I_p$ was obtained using argon as the pressure medium, followed in order by nitrogen, $75N_2$ $25He$, $50N_2$ $50$ $He$, $25N_2$ $75He$, and helium, for all pressures tested. The values of $\Delta I_p$ for the mixed gases, composed of nitrogen and helium, was measured to be between the values for the pure nitrogen and helium. Considering that the expanded uncertainty ($k = 2$) of the calibration values is 40 ppm, the difference between the $\Delta I_p$ values of the different gases exceeds the expanded uncertainty in some conditions. For example, at 50 MPa, $\Delta I_p$ for nitrogen is different from that for argon and helium by more than the expanded uncertainty, 2.0 kPa. Such differences are significant and should be corrected for.
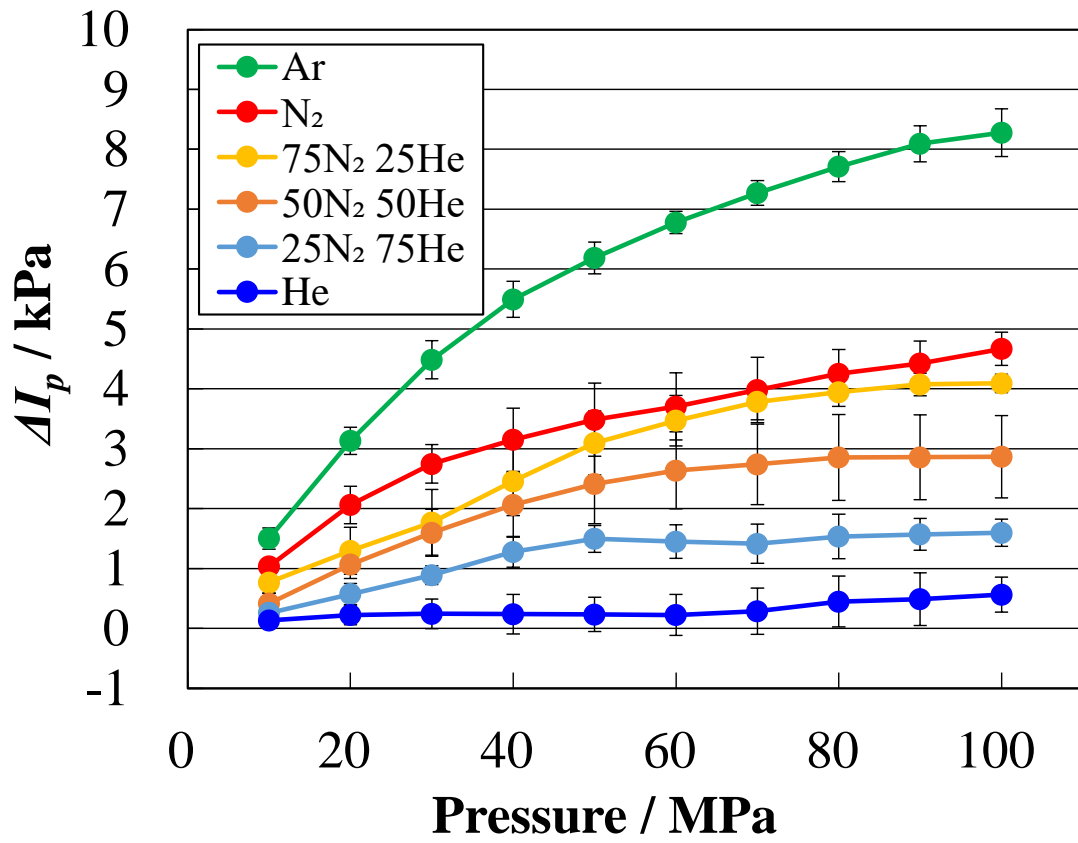
Figure 3.9. Pressure dependence of effects of the pressure medium using six gases. The value of $\Delta I_p$ is dependent on the type of gas as well as the pressure.

### 3.3.3 In-situ measurement of gas density

To evaluate the relationship between the calibration value and the density of the gas, the density of the gas was measured in-situ at each pressure level by measuring head differential pressure [44, 45]. To our knowledge, this is the first attempt to measure the density of high-pressure gas using this method. The density of the gas can be determined using the head difference, the differential pressure, and the local gravity. When the pressure transducer is moved upward using the linear slide, the pressure at the pressure transducer decreases due to the height difference of the pressure transducer before and after being moved. The differential pressure was accurately measured by the pressure balance [45]. By adjusting an additional mass on the pressure balance, the indication of the transducer was set to the same initial value. The differential pressure was calculated from the amount of additional mass required.

The density of the gases was measured at pressures from 10 MPa to 100 MPa at every 10 MPa step. Fig. 3.10 shows the measured value as well as the value from literature [43] of nitrogen. The average value of the ambient temperature was 22.8 °C during the measurements. The literature presents the density value at 23.0 °C. The temperature dependence was included in the uncertainty of the measured density. The difference between the measured value and the literature value is also shown using the right vertical axis. The difference was less than 0.8 kg m$^{-3}$ at all pressures. The error bars indicate the expanded uncertainty ($k = 2$) of the measured density. Table 3.2 presents the uncertainty factors of the density at 100 MPa. The repeatability of measurement was the major source of the uncertainty. The measured and literature values were consistent, within the uncertainty. Therefore, this method can be applied in the measurement of the gas density at ultra high-pressures. The measured densities of the six different gases at each pressure are presented in Fig. 3.11. The density was clearly dependent on the type of gas as well as the pressure. The difference between the measured density of the mixed gas and the density obtained from NIST Reference Fluid Thermodynamic and Transport Properties Database (REFPROP) was less than 3 kg m$^{-3}$. Therefore, it is considered that there is almost no change in the component ratio of mixed gas during the compression process.
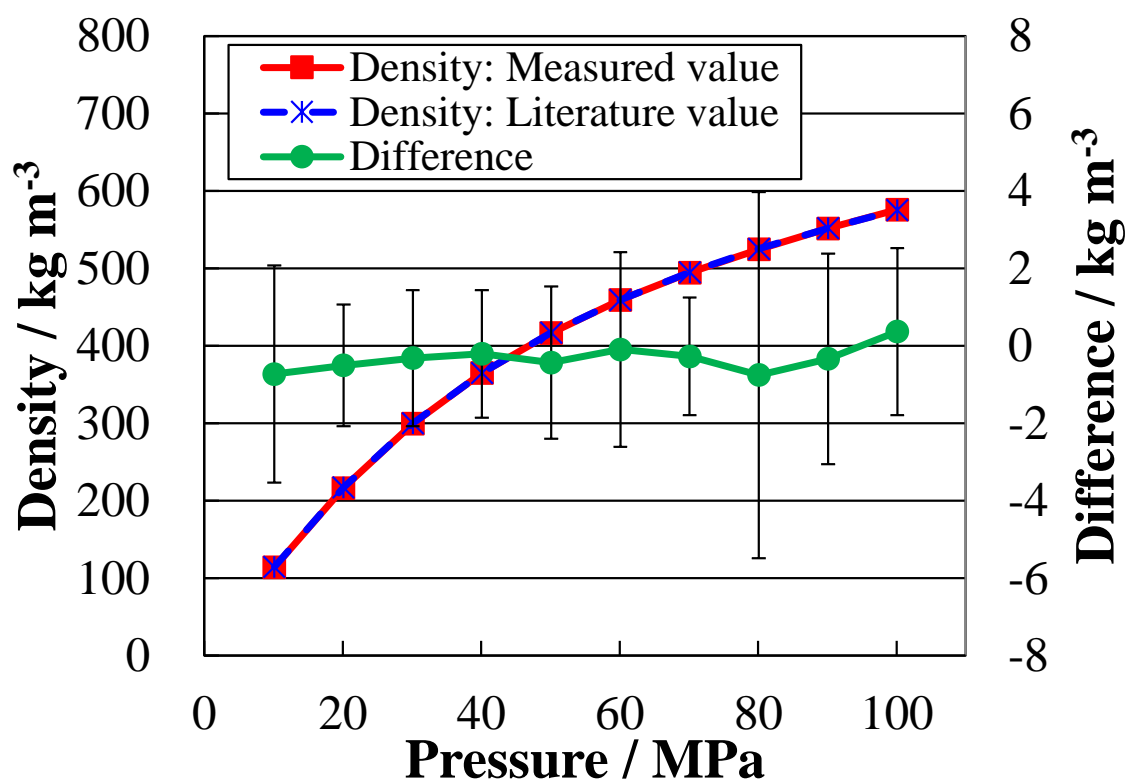
Figure 3.10. Pressure dependence of measured value and literature value of nitrogen density and its difference. The measured and literature values are consistent, within the uncertainty of the measured density.

Table 3.2. Uncertainty factors of measured density of nitrogen at 100 MPa. The repeatability of measurement is the major source of the uncertainty.

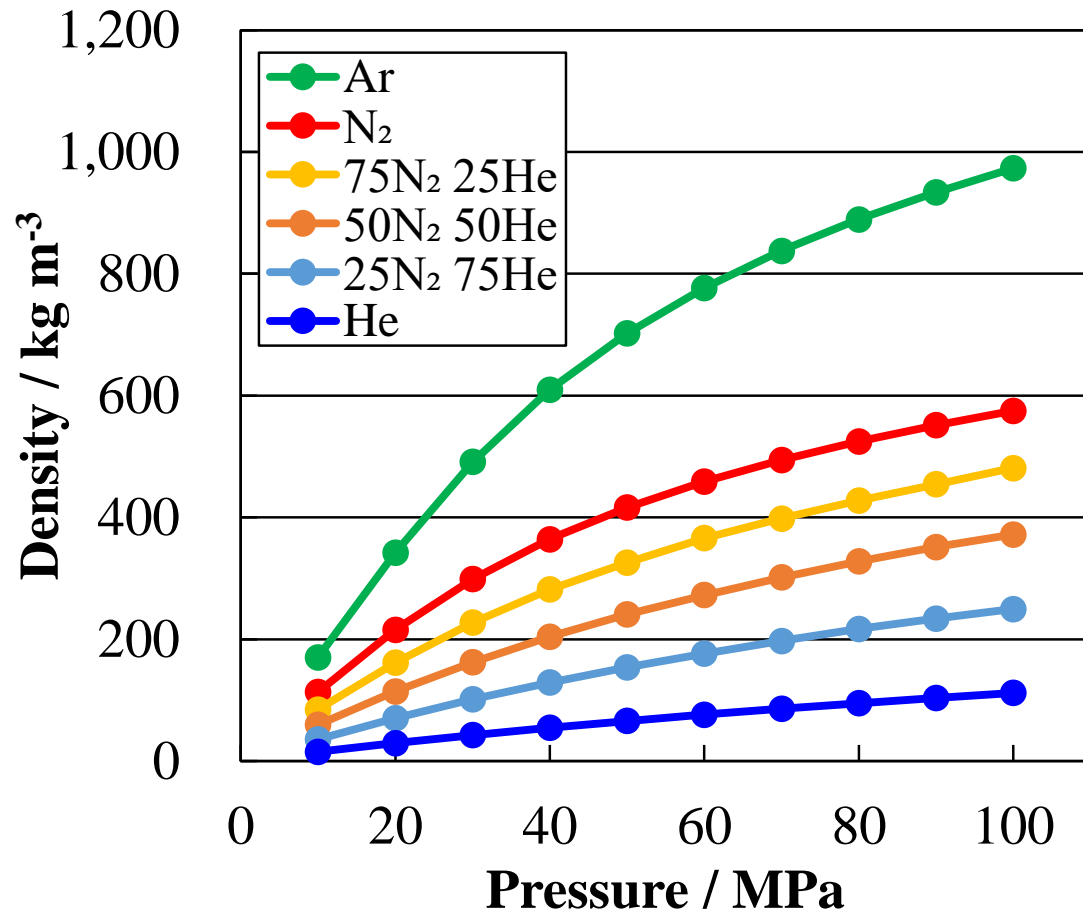| Pressure | 100 MPa |
|---|---|
| Density | 575.8 kg m$^{-3}$ |
| Relative standard uncertainty | $1.8 \times 10^{-3}$ |
| Effective area | $1.8 \times 10^{-5}$ |
| Trim mass | $1.8 \times 10^{-5}$ |
| Sensitivity of pressure balance | $1.0 \times 10^{-3}$ |
| Head difference | $2.0 \times 10^{-4}$ |
| Temperature dependence | $3.4 \times 10^{-4}$ |
| Repeatability | $1.5 \times 10^{-3}$ |
| Relative expanded uncertainty ($k=2$) | $3.7 \times 10^{-3}$ |
| Expanded uncertainty ($k=2$) | 2.1 kg m$^{-3}$ |

Figure 3.11. Pressure dependence of density of six different gases obtained by in-site measurement. The density is clearly dependent on the type of gas as well as the pressure.

## 3.3.4  Relationship between the effects and density

Fig. 3.12 shows the relationship between $\Delta I_p$ and the density of the gas. $\Delta I_p$ and the density of the gas are obtained in section 3.3.2 and 3.3.3, respectively. $\Delta I_p$ was found to be proportional to the density, regardless of the type of gas, including the mixed gases, at each pressure tested. Fig. 3.13 shows the line of best fit when all pressures are combined in one figure. $\Delta I_p$ was also found to be proportional to the density irrespective of the pressure; the slope, $S$, was 8.60 Pa kg$^{-1}$ m$^3$. This result is consistent with the hypothesis that the weight of the gas inside a Bourdon tube affects the indication of the pressure transducer.
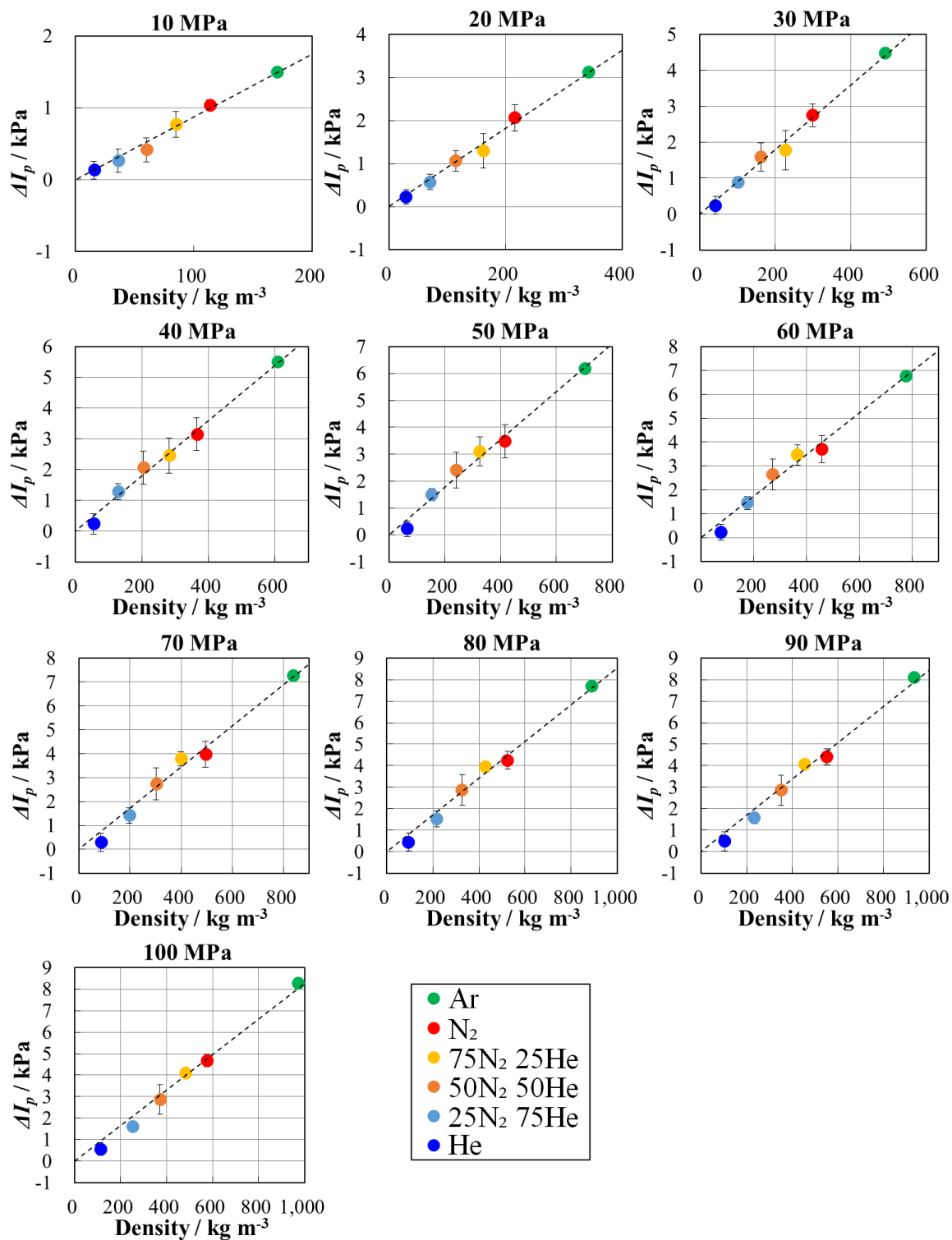
Figure 3.12. Level of variation versus density of pressure medium at each pressure. $\Delta I_p$ was found to be proportional to the density, regardless of the type of gas, including the mixed gases, at each pressure tested.
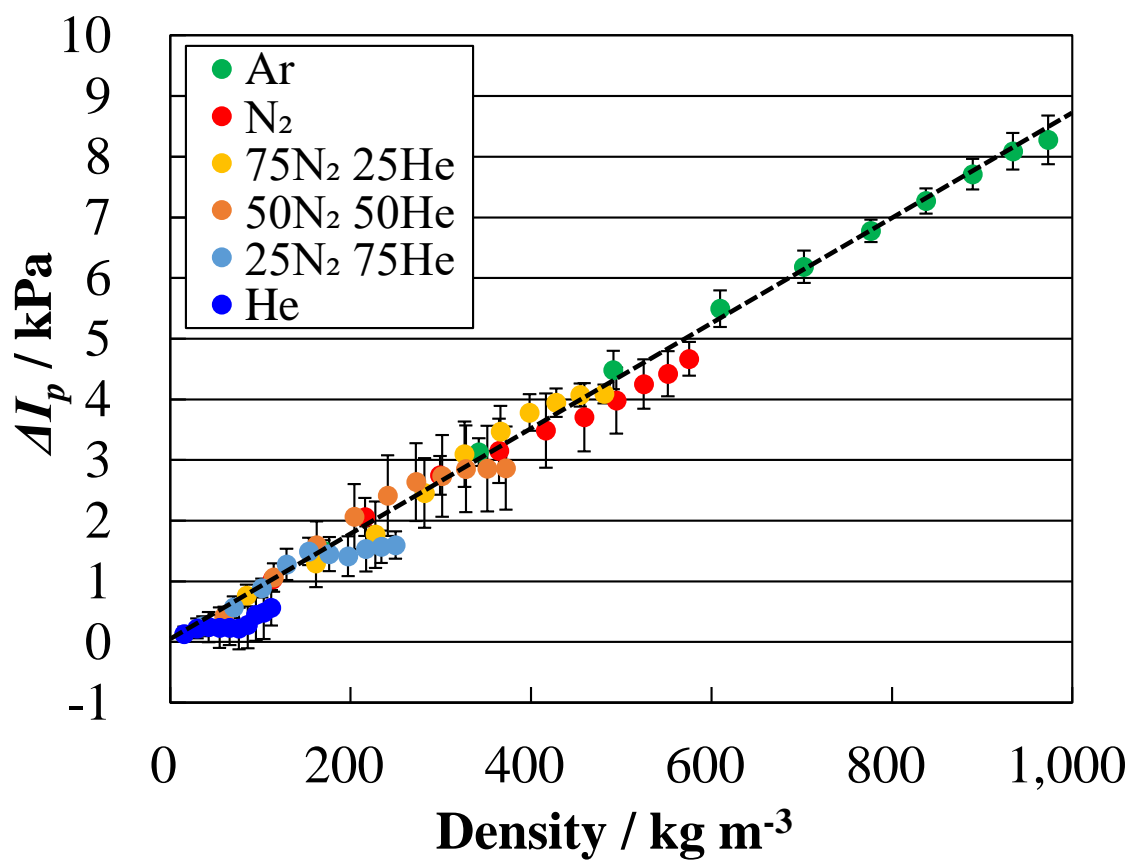
Figure 3.13. Level of variation versus density of pressure medium including all pressures. $\Delta I_p$ was found to be proportional to the density irrespective of the pressure

# 4. Methods for reducing effects and estimation of calibration value from gas density

## 4.1 Adjusting orientation of the pressure transducer

Since the quartz Bourdon-type pressure transducer was affected by the type of gas and the orientation, it is recommended that the transducers are used with the same pressure medium and the same orientations as they were calibrated. Based on the evaluation results in section 3, the methods for reducing the effects of the type of gas and correcting the calibration values based on the gas density are discussed in section 4. Two methods for reducing the effect of the type of gas are discussed in this section.

As discussed in section 3, when the rotation angle of the pressure transducer is $\theta_0$, the calibration values of the pressure transducer is expected to be not affected by the type of measuring gas. Although it is impossible to identify the direction of the Bourdon tube in the sensing element from the transducer's outer appearance, it can be estimated from the evaluated relation between the rotation angle and the calibration value. When the rotation angle is $\theta_0$, it is expected that the direction of the deformation of the Bourdon tube is perpendicular to the direction of gravitational force.

Horizontally oriented pressure transducer A at rotation angle $\theta_0$, identified as 280° from Fig. 3.5 (c), was calibrated by using nitrogen and by using helium, and the calibration results were shown in Fig. 4.1 (a). The difference in calibration value depending on the type of gas is within the standard deviations. Fig. 4.1 (a) also shows $R_{p,\theta_0}$ as obtained by fitting $R_{p,\theta}$ from Fig. 3.4 (a). $R_{p,\theta_0}$ was also consistent with the actual calibration values at rotation angle $\theta_0$.

Pressure transducer A was also calibrated at rotation angle $\theta_0 + 90°$, at which the calibration values are strongly affected by the type of gas and the calibration results by using nitrogen and helium were shown in Fig. 4.1 (b). The difference in the calibration values between nitrogen and helium was about 2.0 kPa at 100 MPa. The difference was comparable to the uncertainty of the calibration value.

From the above results, it was shown that when the quartz Bourdon-type pressure transducer is oriented horizontally, the effect of the type of gas can be reduced by adjusting the rotation angle of the pressure transducer.
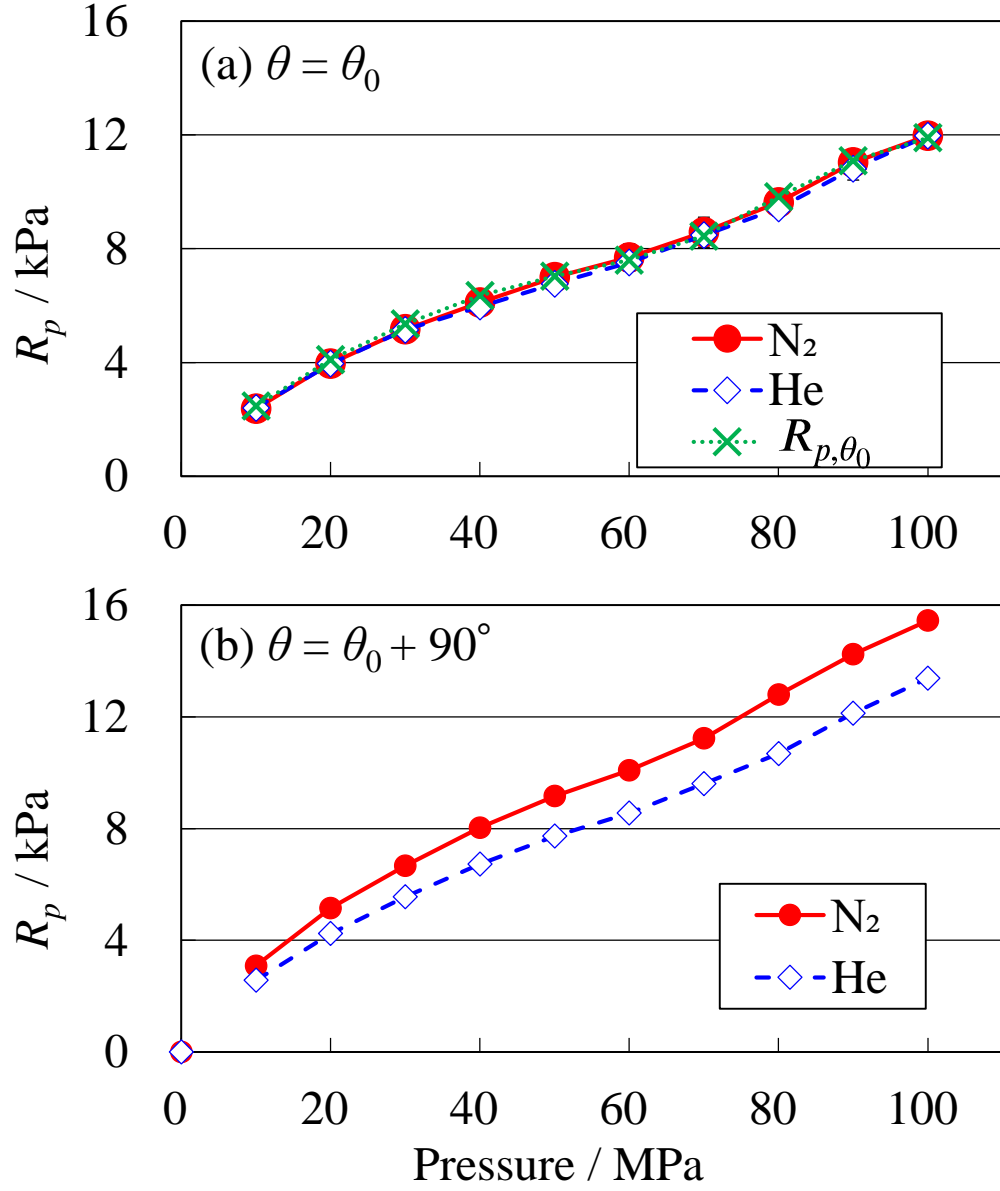
Figure 4.1. Calibration values of pressure transducer A at rotation angles (a) $\theta_0$ and (b) $\theta_0 + 90°$ when using nitrogen and those when using helium. $R_{p,\theta_0}$ is obtained in Fig. 3.4 (a). The effect of the type of gas can be reduced by adjusting the rotation angle of the pressure transducer.

When the transducer is oriented vertically, the deformation of the Bourdon tube by the gravitational force arising from the weight of the pressure medium at the upward is opposite to that at the downward. Therefore, it is thought that the effect of the weight of the pressure medium can be eliminated by averaging the calibration values at the upward and downward orientations.

Fig. 4.2 shows the average value of $R_p$ at the upward and downward orientations, $R'_p$ in Eq. (3.6). The pressure medium was both nitrogen and helium. The average values using nitrogen and those using helium showed good agreement. The calibration values of the horizontally oriented transducer at rotation angle $\theta_0$, $R_{p,\theta_0}$, with nitrogen and with helium are also shown. Each value showed good agreement within 0.6 kPa at all measurement pressure. It was comparable to the standard deviations of the calibration value. The average value, $R'_p$ agreed well with $R_{p,\theta_0}$ because both values only include the contribution purely from the applied pressure. The effect of the type of gas on the calibration value can be reduced by averaging the calibration values at the upward and downward orientations, or adjusting the orientation of the transducers oriented horizontally.
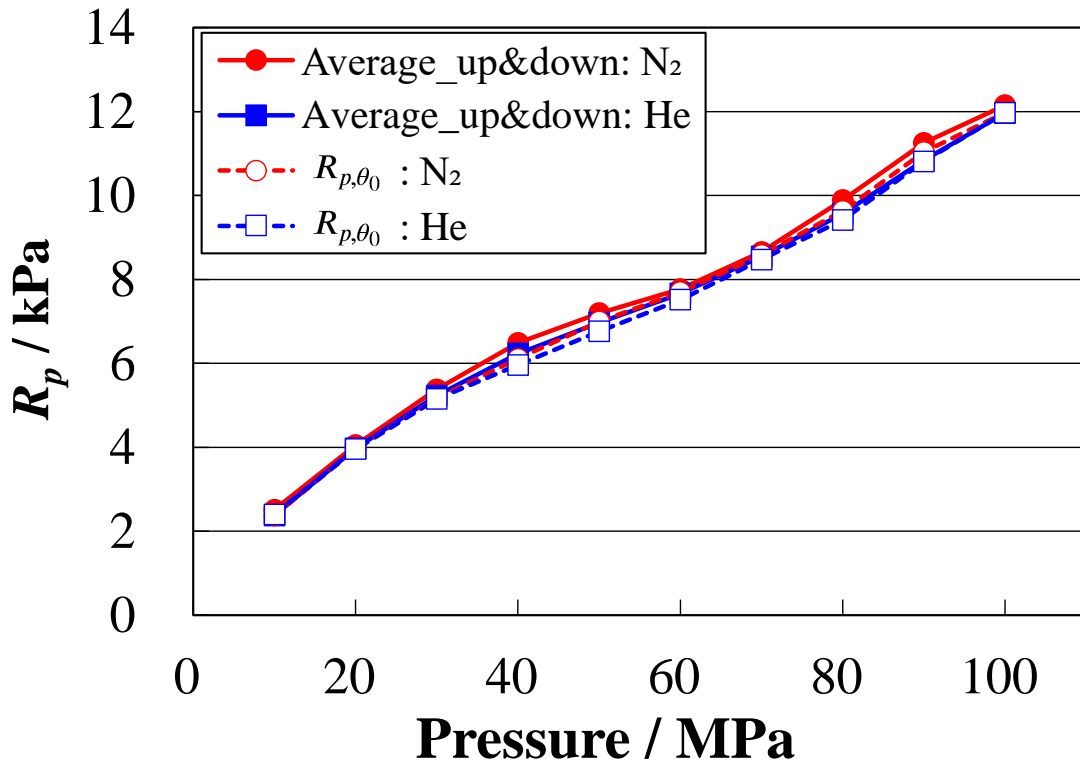


Figure 4.2. Average values of calibration values at upward and downward orientations. The average values are independent on the type of gas. Calibration values at horizontal orientations with rotation angle $\theta_0$, $R_{p,\theta_0}$. Each value showed good agreement within the standard deviations.

## 4.2   Using two pressure transducers

We will discuss about the case that two pressure transducers can be used for measurements. It is thought that the effect of the type of gas also can be reduced by averaging the calibration values of two transducers at the upward and at the downward. In addition, when the sensing elements of the two pressure transducers are arranged in point symmetry with each other, the deformations of the two Bourdon tubes by the gravitational force arising from the weight of the pressure medium are opposite to each other in any orientation. Therefore, it is thought that the effects of both the type of gas and the orientation also can be reduced by averaging the calibration values of the arranged two transducers.

Fig. 4.3 shows a point-symmetry arrangement of two pressure transducers. The inlet port of two transducers #1 and #2 at rotation angle $\theta_0$ were arranged face to face with each other. This posture was defined as $\theta = 90°$, $\varphi = 90°$. Rotation angle $\theta_0$ of each pressure transducer were evaluated beforehand by the method in section 3.2.
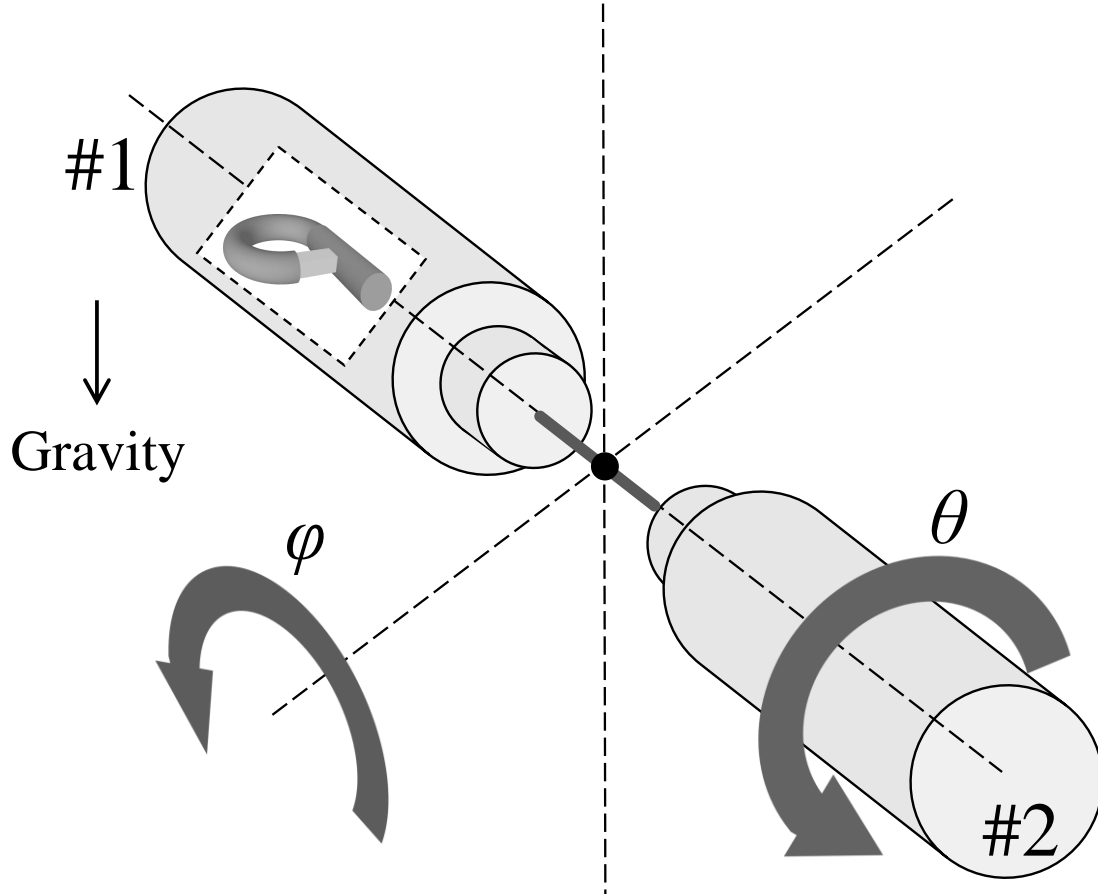


Figure 4.3. Two pressure transducers at rotation angle $\theta_0$ are positioned in point symmetry with each other. This posture is defined as $\theta = 90°$, $\varphi = 90°$.

The set of two transducers arranged in point symmetry were oriented vertically ($\varphi = 0°$ and $180°$), and calibrated both with nitrogen and with helium. The rotation angle $\theta$ was fixed to $90°$. When $\varphi = 0°$, transducer #1 was oriented upward and transducer #2 was oriented downward. When $\varphi = 180°$, transducer #1 was oriented downward and transducer #2 was oriented upward. The calibration value, $R_p$ of the two transducers were averaged. Fig. 4.4 shows the average value of the two transducers, $R_{p,\text{ave}}$, both with nitrogen and with helium at $\varphi = 0°$ and $180°$. At the same orientation, $R_{p,\text{ave}}$ with nitrogen and $R_{p,\text{ave}}$ with helium showed good agreement within 0.7 kPa in all measurement pressure, relatively $7.0 \times 10^{-6}$ of full scale. It was comparable to the standard deviations of the calibration value. In addition, $R_{p,\text{ave}}$ at $\varphi = 0°$ and $180°$ showed good agreement with both gases. As described in section 3.2, when the pressure transducer was oriented vertically, the calibration value significantly differed between the upward and downward orientations, and also differed between nitrogen and helium. From the above results, however, the both effects were reduced by averaging the output values of the two pressure gauges arranged in point symmetry.
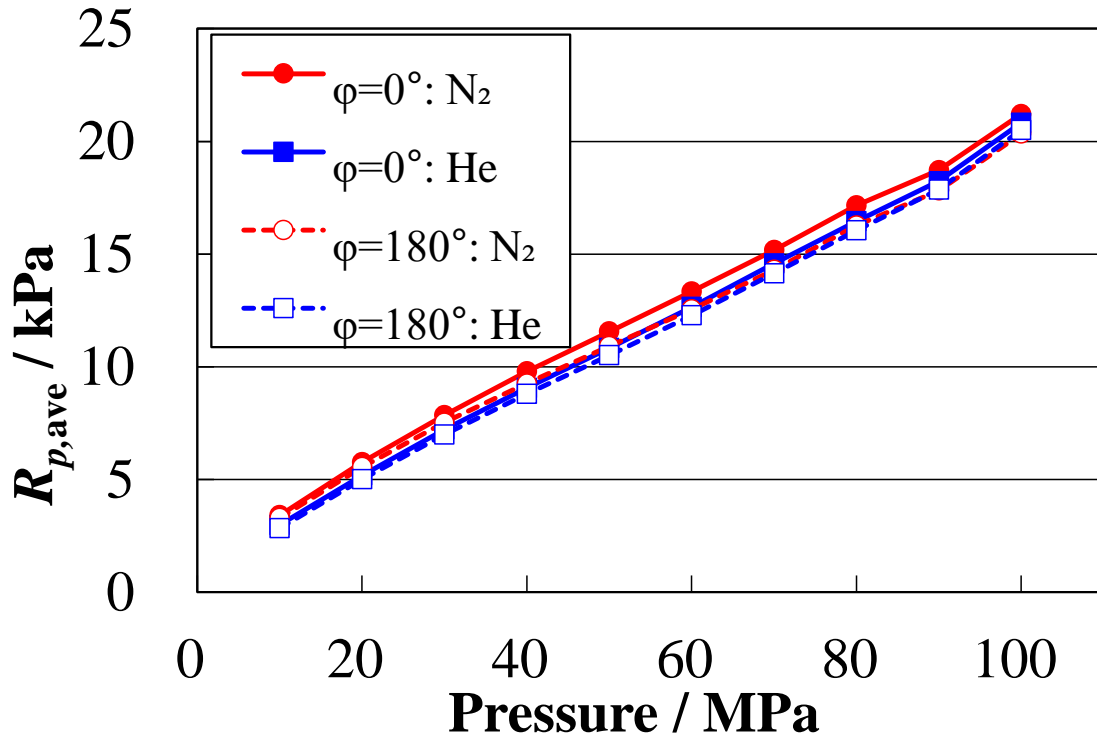


Figure 4.4. Average value of two transducers, $R_{p,\text{ave}}$, at $\varphi = 0°$ and $180°$ both with nitrogen and with helium. Each value showed good agreement within the standard deviation.

The effect of the orientation of the pressure transducer is evaluated in detail. Two transducers #1 and #2, arranged in point symmetry was calibrated at different orientation. The pressure medium was nitrogen. In the first experiment, the rotation angle $\varphi$ was fixed to 90°. The rotation angle $\theta$ was changed in order of 90°, 45°, 0°, 90°, 135°, 180°, 90°. Figure 4.5 (a) shows the calibration values at 100 MPa, $R_{100}$, of transducer #1 and #2 at each rotation angle $\theta$. The average values of the two transducers are also shown. The three $R_{100}$ at $\theta = 90°$ showed good agreement within 0.5 kPa in both transducer #1 and #2. Although the maximum difference by the rotation angle $\theta$ of transducer #1 was 7.2 kPa and transducer #2 was 7.0 kPa. The maximum difference of the average values was 0.5 kPa and, the average values were not affected by the rotation angle $\theta$.

In the second experiment, the rotation angle $\theta$ was fixed to 90°. The rotation angle $\varphi$ was changed in order of 90°, 45°, 0°, 90°, 135°, 180°, 90°. Fig 4.5 (b) shows $R_{100}$ of transducer #1, #2 at each rotation angle $\varphi$. The average values of the two transducers are also shown. The three $R_{100}$ at $\varphi = 90°$ showed good agreement within 0.5 kPa in both transducer #1 and #2. Although the maximum difference by rotation angle $\varphi$ of transducer #1 was 7.8 kPa and transducer #2 was 9.5 kPa, the average values was 1.0 kPa. In both cases that changing $\theta$ and changing $\varphi$, the effect of the orientation on the calibration value was able to be reduced by averaging the calibration values of the arranged two transducers.

When the sensing elements of two pressure transducers were arranged in point symmetry, the average values of two transducers were almost independent of both the type of gas and the orientation. If two transducers having the same effects are used, the average values would be completely independent of both the type of gas and the orientation. In this study, the inlet ports of two transducers were arranged face to face with each other. However, the same results can be obtained as long as the sensing elements are arranged in point symmetry with each other.
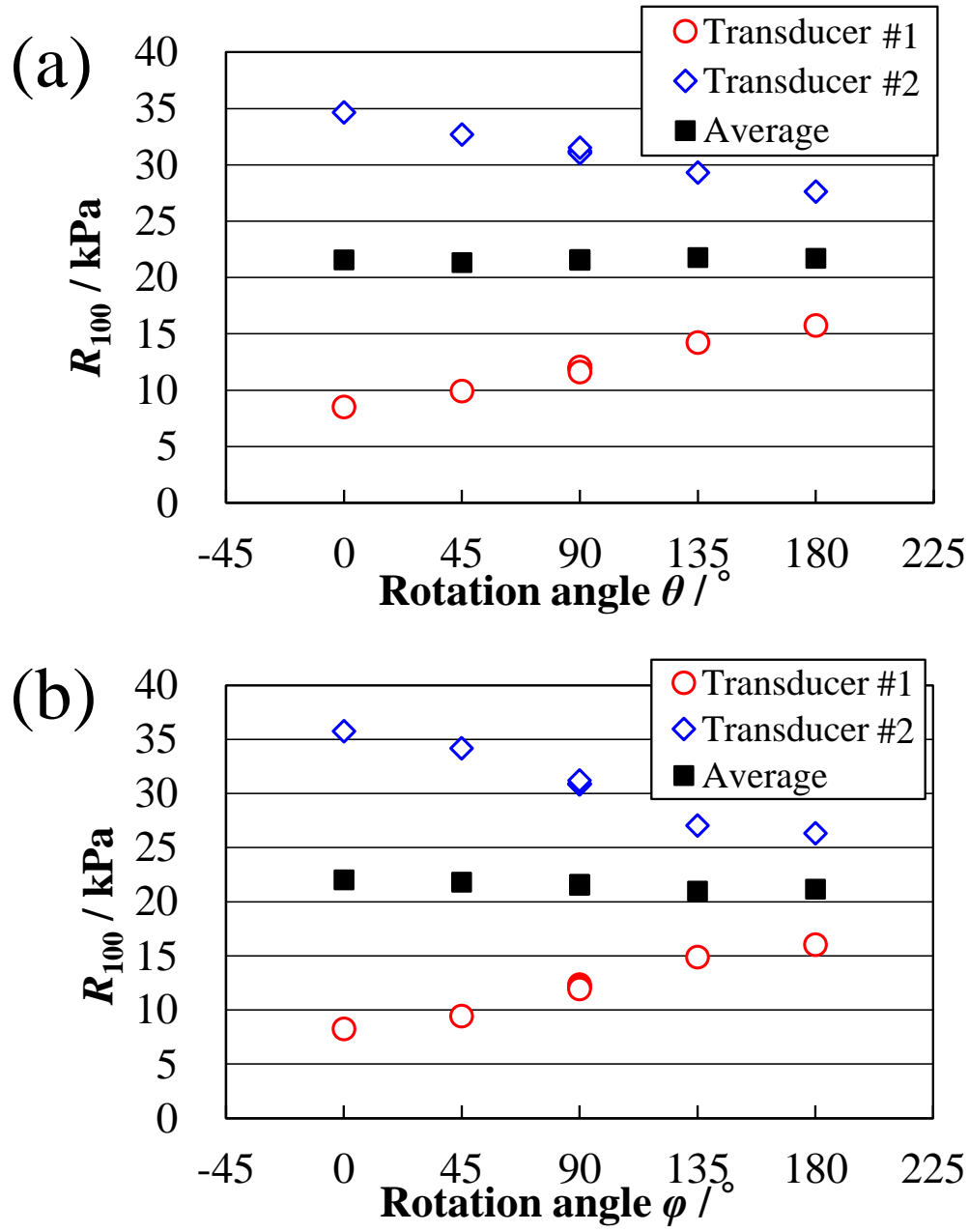
Figure 4.5. Calibration values at 100 MPa, $R_{100}$, of transducer #1 and #2 (a) at different rotation angles $\theta$, (b) at different rotation angles $\varphi$. The average values of the two transducers are also shown. The effect of the orientation on the calibration value was able to be reduced by averaging the calibration values of the arranged two transducers.

## 4.3  Estimation of calibration value from gas density

In section 3.3, the effect of type of gas was found to be proportional to the density, regardless of the type of gas and pressure. From the slop, $S$, of the relationship between the effects and density in Fig. 3.13, the calibration values of any gas can be corrected using their density. We discuss a method for correcting the calibration value of the pressure transducer according to the type of measuring gas when the transducer is oriented vertically. Here, we consider the case where a calibrated pressure transducer is used with a gas not used in calibration process. When the pressure transducer is oriented upwards, the estimated calibration value of a gas at the pressure $p$, $R_{p,\mathrm{meas}}$, can be expressed by the following equation,

$$R_{p,\mathrm{meas}} = R_{p,\mathrm{cal}} - S \cdot (\rho_{p,\mathrm{meas}} - \rho_{p,\mathrm{cal}}), \qquad (4.1)$$

where $R_{p,\mathrm{cal}}$ is the calibration value of the gas used in the calibration process, $\rho_{p,\mathrm{cal}}$ and $\rho_{p,\mathrm{meas}}$ are the densities of the gas used in the calibration process and during the measurement, respectively. When the pressure transducer is oriented downwards, the sign of the second term becomes positive because the direction of the gravitational force on the Bourdon tube from the weight of the gas has been inverted [19, 20].

As an example of the correction and uncertainty evaluation, we estimated the calibration value of hydrogen using the value of nitrogen. In this scenario, the value of the second term of Eq. (4.1) is 4.5 kPa at 100 MPa, using the parameters detailed in Table 4.1(a). The value from the literature [46] is used for the density of hydrogen. Thus, the calibration value of hydrogen at 100 MPa is estimated to be 4.5 kPa larger than the value of nitrogen. The standard uncertainty of the slope is 0.08 Pa kg$^{-1}$ m$^3$; the standard uncertainty of the density is the average value of the standard uncertainty of the measured density in section 3.3.3, 1.2 kg m$^{-3}$. Therefore, the standard uncertainty for the correction is determined to be 4.5×10$^{-2}$ kPa at 100 MPa as shown in Table 4.1(b). The additional uncertainty for the correction is sufficiently smaller than the standard uncertainty of the calibration value, 2.0 kPa. Thus, once the relationship has been determined, the calibration values of any gas can be estimated using its density, without any substantial increase in the uncertainty.

Table 4.1. Correction of calibration value for hydrogen based on that for nitrogen. (a) Parameters used for correction. (b) Uncertainty evaluation of calibration value (hydrogen). The uncertainty for the correction is sufficiently smaller than the standard uncertainty of the calibration value.

(a)

|  | Value | Uncertainty |
|---|---|---|
| Slope / Pa kg$^{-1}$ m$^3$ | 8.60 | 0.08 |
| Density of gas used in measurement (hydrogen) / kg m$^{-3}$ | 49.7 | 1.2 |
| Density of gas used in calibration (nitrogen) / kg m$^{-3}$ | 575.8 | 1.2 |

(b)

| | |
|---|---|
| Standard uncertainty of calibration value (nitrogen) | 2.0 kPa |
| Standard uncertainty for correction | $4.5 \times 10^{-2}$ kPa |
| Slope | $4.2 \times 10^{-2}$ kPa |
| Density of gas used in measurement (hydrogen) | $1.0 \times 10^{-2}$ kPa |
| Density of gas used in calibration (nitrogen) | $1.0 \times 10^{-2}$ kPa |
| Combined standard uncertainty | 2.0 kPa |
| Expanded uncertainty ($k = 2$) | 4.0 kPa |

# 5. Conclusions

The purpose of this study is an establishment of the reliable and high precision pressure measurement of ultra high-pressure gas, which has been in increasing demand in recent years. To perform precision pressure measurements, it is necessary to periodically calibrate the pressure gauges and understand their characteristics. However, the measurement standard was not established, and detailed characterization of the pressure gauges was not performed. In this study, we have obtained three fruitful results, development of a pressure calibration system for ultra high-pressure gas, clarification of the effect of type of measuring gas, and methods for reducing the effect, which are summarized as follows.

A pressure calibration system for ultra high-pressure gas was developed by using a liquid-lubricated pressure balance as a standard device. In the developed calibration system, the pressure gauges can be calibrated at pressures up to 100 MPa. The liquid-lubricated pressure balance was characterized and the standard uncertainty of generated pressure at 100 MPa was estimated as $1.8 \times 10^{-5}$. A pressure gauge was calibrated at pressures up to 100 MPa by using the developed calibration system. The calibration results of the pressure gauge were compared with the calibration results of same pressure gauge obtained from an existing hydraulic pressure calibration system. The calibration results from both calibration systems showed good agreement within the uncertainty of the calibration results from the developed calibration system. From this result, the validity of the developed calibration system was confirmed. The measurement standard of gas pressures up to 100 MPa has been established. International equivalence of the pressure standard is also ensured by an international comparison. The developed calibration system should contribute to ensuring the reliability of the gas pressure measurements at pressures up to 100 MPa.

The fall rate of the liquid-lubricated piston-cylinder was measured for characterization and depended on the pressure transmitting medium. The fall rate of the piston is an important characteristic for operating pressure balances. When the liquid-lubricated piston-cylinder generated gas pressure, the fall rate was affected by gas dissolution into the liquid inside the piston-cylinder assembly. Since the piston fall rate significantly changed with elapsed time from applying pressure, the liquid-lubricated pressure balance needed to be handled with care. To investigate the effect of temperature changes on the calibration, the gas temperature inside the piping was measured by a thermocouple. When the pressure was changed from 0 MPa to 10 MPa, the temperature rapidly increased from 24.0 °C to 26.3 °C immediately after the start of pressurization. Then the temperature exponentially dropped when the pressurization speed became slow. The temperature returned initial values within a few minutes after the pressure change and the temperature during data sampling in the calibration was sufficiently stable. Therefore, the effects of temperature change on the calibration were negligible in the developed calibration system.

To perform precision pressure measurements, it is necessary to understand characteristics of the pressure gauges. The effect of pressure medium on quartz Bourdon-type pressure transducers was investigated by using the developed calibration system. It was found that the calibration values of the pressure transducers were affected by the type of measuring gas. The effects could not be neglected for

precision measurement. Since the pressure transducers are used in a variety of applications and measure the pressure of different gas, the effect of the type of gas on the calibration values is important characteristics. The reason why the indication of the pressure transducer differs depending on the type of gas was investigated with a focus on the density of the gas and the structure of a sensing element. We thought that the effect was related to the weight of measuring gas inside the sensing element. The weight can cause extensional or compressional deformation of the Bourdon tube in the sensing element by gravitational force in addition to the deformation due to the applied pressure. Since the density of ultra high-pressure gas largely differs depending on the type of gas, the gravitational force differs depending on the type of gas. Therefore, the indication of the pressure transducer is affected.

Based on the above considerations, the indications depend on both the type of gas and the orientation of the pressure transducer. It was expected that the indication of the pressure transducer depended on the rotation angle of the transducer oriented horizontally because the direction of gravitational force received by the sensing element was changed with the rotation angle. When the transducer was oriented vertically, it was expected that the effects was opposite for the upwards and downwards orientations. To confirm the above assumption experimentally, the effect of the orientations of the transducer on the calibration value were evaluated. The effect of the orientation was consistent with the above assumption. When the transducer was oriented horizontally, the calibration was expressed using a sinusoidal curve against the rotation angle. The effects of the type of gas was opposite for the upwards and downwards orientations. The effects of the orientation and the type of gas could not be neglected for high precision measurement.

Based on the above considerations, it was also expected that the level of variation was correlated with the density of gas in the Bourdon tube. We determined the level of variation in the pressure transducer caused by using different measuring gas. Six gases with different densities: argon, nitrogen, helium, and three types of mixed gases composed of nitrogen and helium were used to evaluate the level of variation for a wide range of densities. The level of variation in the calibration value was determined using the difference between the calibration values of the pressure transducer obtained while oriented vertically upwards and downwards. The level of variation was found to be dependent on the type of gas as well as the pressure. Because the density in actual measurement condition was necessary for evaluating the relationship between the level of variation and the gas density, the density of ultra high-pressure gas was measured in-situ for each pressure by measuring head differential pressure. The expanded uncertainty ($k = 2$) of the measured nitrogen density was estimated as 2.1 kg m$^{-3}$ at 100 MPa. The repeatability of the measurement was the major factor in the uncertainty. The measured values and the literature values of nitrogen were consistent within the uncertainty. Therefore, this measurement method can be applied in the measurement of the gas density at ultra high-pressures. The density of six gases was measured in-situ using this method. The level of variation was proportional to the density of the gas, regardless of the type of gas and pressure. This result is consistent with the hypothesis that the weight of the gas inside the Bourdon tube affects the indication of the transducer. The slope of the line of best fit for the data was calculated to be 8.60 Pa kg$^{-1}$ m$^3$.

Such effects were significant and should be reduced or corrected for. The methods for reducing the effects of the type of gas were discussed. When the direction of the deformation of the Bourdon tube was perpendicular to the direction of gravitational force, it was thought that the calibration values of the transducer were not affected by the type of gas. The orientation of the Bourdon tube, which cannot be identified from the outer appearance of the transducer, was experimentally identified. It was shown that the calibration values when using nitrogen and those when using helium agreed well when the transducer was oriented at the identified rotation angle. When the transducer was oriented vertically, since the deformation of the Bourdon tube by the gravitational force arising from the weight of the pressure medium at the upward was opposite to that at the downward, the effect of the type of gas was able to be reduced by averaging the calibration values at the upward and downward orientations. In addition, the effects of the type of gas were reduced by averaging the calibration values of two transducers at the upward and at the downward. When the sensing elements of the two pressure transducers were arranged in point symmetry with each other, the deformations of the two Bourdon tubes by the gravitational force arising from the weight of the pressure medium were opposite to each other in any orientation. Therefore, the effects of both the type of gas and the orientation were able to be reduced by averaging the calibration values of the arranged two transducers. The maximum difference of the calibration values of the pressure transducer by the orientation was 9.5 kPa. However, the maximum difference of the average values of the arranged two transducers by the orientation was 1.0 kPa. If two transducers having the same effects are used, the average values would be completely independent of both the type of gas and the orientation. Using the slope of the relationship between the effect and the density of gas, the calibration values can be estimated from the density of gas. We estimated the calibration value of hydrogen using the known values for nitrogen. The additional uncertainty for the correction was sufficiently smaller than the uncertainty of the calibration value. Thus, the total uncertainty of the estimated value was comparable to the uncertainty of the calibration value of nitrogen. Therefore, once the relationship was determined, the calibration values of any gas can be estimated using their density, without a substantial increase in the uncertainty.

We developed a calibration system that can calibrate pressure gauges of ultra high-pressure gas and evaluated its characteristics, and established the measurement standard of gas pressures up to 100 MPa for the first time. International equivalence of the established pressure standard was ensured by an international comparison. We have found that the output value of a quartz Bourdon-type pressure transducer is affected by the type of measuring gas, and clarified for the first time in the world that the reason is related to the gravitational force arising from the weight of measuring gas. Methods for reducing the effect of the type of measuring gas were devised, and its effectiveness was demonstrated. This research contributed to establish the reliable and high precision pressure measurement of ultra high-pressure gas.

# References

[1]  T. Kobata et al., *Synthesiology - English edition* **4**-4 (2012) 221-226.

[2]  UN/ ECE, Global technical regulation No. 13: Global technical regulation on hydrogen and fuel cell vehicles (2013)

[3]  NIST Handbook 44, 2013 Edition: Specifications, Tolerances, and other Technical Requirements for Weighing and Measuring Devices. Section 3.39: Hydrogen Gas-Measuring Devices - Tentative Code (2013)

[4]  EMRP Call 2013 - Energy and Environment: SRT-g05; Metrology for hydrogen transport (2013)

[5]  N. Sakoda et al., *International Journal of Hydrogen Energy* **41** (2016) 17169-17174.

[6]  The BIPM key comparison database (https://www.bipm.org/kcdb/)

[7]  S. W. Doty et al., *Proc. of the 1995 Measurement Science Conference* (1995)

[8]  H. Iizumi et al., *Measurement* **102** (2017) 106 -111.

[9]  T. Kobata, *Metrologia* **42** (2005) S235.

[10]  H. Kajikawa et al., *Meas. Sci. Technol.* **21** (2010) 065104.

[11]  I. Kocas et al., *Measurement* **45** (2012) 2486-2489.

[12]  M. Kojima et al., Metrologia 52 (2015) 262-266.

[13]  JIS B7547-1, -2 (2020).

[14]  W. W. Chadwick Jr. et al., *Journal of Volcanology and Geothermal Research* **150** (2006) 313–327.

[15]  Paroscientific, Inc., User's Manual for Digiquartz Broadband Intelligent Instruments with Dual RS-232 and RS-485 Interfaces (2013).

[16]  Paroscientific, Inc., User's Manual for Model 735 Intelligent Display And Model 745 High Accuracy Laboratory Standard (2009).

[17]  Fluke calibration, RPM4 Operation and Maintenance Manual (2012).

[18]  H. Iizumi et al., *Measurement* **131** (2019) 358-361.

[19]  H. Iizumi et al., *ACTA IMEKO* **8 (3)** (2019) 25-29.

[20]  H. Iizumi et al., *Journal of Physics: Conference Series* **1065** (2018) 162008

[21]  H. Kajikawa et al., *Metrologia* **53** (2016) 03002.

[22]  OIML R 110 (1994).

[23]  JIS B7610 (2012).

[24]  JIS B7616 (2013).

[25]  EAL-G26 (1997).

[26]  S. Lewis et al., *The Pressure Balance: A Practical Guide to its use*, National Physical Laboratory (1979).

[27]  B. Fellmuth et al., *C. R. Physique* **10** (2009) 828-834.

[28]  J. W. Schmidt et al., *Metrologia* **36** (1999) 525-529.

[29]  P. L. M. Heydemann et al., *Experimental Thermodynamics Vol II*, (1975) 147-202.

[30]  T. Kobata et al., *Trans. of the Society of Instrument and Control Engineers* **39**-4 (2003) 349-356.

[31] H. Kajikawa et al., *Rev. Sci. Instrum*. **80** (2009) 095101.

[32] R. S. Dadson et al., *Metrologia* **1** (1965) 55-68.

[33] W. Sabuga et al., *Metrologia* **43** (2006) 311-325.

[34] T. Kobata, *Metrologia* **46** (2009) 591-598.

[35] P. Delajoud et al., *Proc. of International Symposium on Pressure and Vacuum (IMEKO TC16)* (2003) 154-159.

[36] W. Sabuga et al., *Metrologia* **42** (2005) 07005.

[37] T. Kobata et al., *Metrologia* **42** (2005) 07006.

[38] T. Kobata et al., *Metrologia* **42** (2005) S231-S234.

[39] ISO/IEC 2008 Guide 98-3 *Guide to the expression of Uncertainty in Measurement* (GUM: 1995).

[40] P. R. Stuart, *Metrologia* **30** (1994) 727-735.

[41] ISO/IEC Guide 98-3:2008 (2008)

[42] JIS B7505-1 (2017).

[43] R. Span, et al., *J. Phys. Chem. Ref. Data* **29** (2000) 1361-1433.

[44] T. Kobata et al., *Measurement* **131** (2019) 79-84.

[45] H. Kajikawa et al., *Proceedings of the SICE Annual Conference 2017* (2017) 1604-1606.

[46] J. Leachman et al., *J. Phys. Chem. Ref. Data* **38** (2009) 721-748.

# Acknowledgements